Glial cell activation and re-expression of putative myelinating inhibitors in the brain of mouse model for demyelinating disease

Michio Matsumoto

Doctor of Philosophy

Department of Physiological Sciences,

School of Life Sciences,

The Graduate University for Advanced Studies

2003

Contents

Abbreviations

CNS	central nervous system
DAB	3,3’-diaminobenzidine tetrahydrochrolide
DMEM/F12	Dulbecco’s modified eagle’s medium: nutrient mixture F-12
E	embryonic days
EGFP	enhanced green fluorescent protein
bFGF	basic fibroblast growth factor
GFAP	glial fibrillary acidic protein
GFP	green fluorescent protein
HE	hematoxylin and eosin
Ig	immunoglobulin
ISH	in situ hybridization
KB	Kluver-Barrera's
LFB	luxol fast blue
MBP	myelin basic protein
M-CSF	macrophage colony-stimulating factor
mRNA	messenger ribonucleic acid

MS	multiple sclerosis
NCAM	neural cell adhesion molecules
OL	oligodendrocyte
OLP	oligodendrocyte progenitor
PB	phosphate buffer
PBS	phosphate-buffered saline
PLP	proteolipid protein
PMD	Pelizaeus Merzbacher disease
PSA	polysialic acid

Abstract

Overexpression of the proteolipid protein (PLP) gene, which is the major component of central nervous system myelin, causes unique demyelinating disorder in mice (*Plp/-* mouse). In this transgenic animal model, normal-appearing myelin is formed at an early stage of their life and late-onset chronic demyelination occurs after several months. I aimed to understand the molecular mechanisms underlying this neuropathology. I first demonstrated that remyelination is severely affected in the aged *Plp/-* mouse. This was not caused by the deprivation of oligodendrocyte progenitors, expressing Olig1, Olig2 and Sox10, because they were present at a higher number in the central nervous system of mutant mice than in the wild type control throughout their lives. These suggested that oligodendrocyte progenitors cannot differentiate or mature due to a change in the microenvironment. I then searched for factors inhibiting oligodendrocyte development. I observed up-regulation of PSA-NCAM and cystatin C expression, both of which have been reported to be inhibitory for oligodendrocyte development and are produced by non-oligodendroglial cells. Thus I investigated the change in the number and properties of astrocytes and microglia. Glial activation was observed much earlier than the active

demyelinating period. These data imply that not only cell intrinsic mechanisms but also extrinsic mechanisms contribute to the defect in re-myelination in the PLP overexpressing brain. During demyelination, resident microglial cells and astrocytes become activated, astrogliosis occurs, and these cells may change the environment to that inhibitory for oligodendrocyte differentiation/maturation.

Introduction

Oligodendrocytes are the glial cells that form myelin in the central nervous system (CNS). The function of myelin is to enhance nerve conduction along the axons. The myelin membrane comprises approximately 80% lipids and 20% proteins. Among myelin proteins, proteolipid protein (PLP) constitutes about 50% of the protein mass of mature CNS myelin and is an integral membrane protein, thought to span the lipid bilayer four times (Griffiths et al., 1998).

Mutations within the *PLP* gene in human cause Pelizaeus-Merzbacher disease (PMD; MIM 312080), a CNS dysmyelinating disease typically characterized by nystagmus, delayed psychomotor development, spasticity, and ataxia. Some *PLP* gene mutations cause the milder syndrome X-linked spastic paraplegia (SPG2; MIM 312920) (Hodes et al., 1993; Griffiths et al., 1998). Both conditions are caused by alterations in the coding region of *PLP*. In addition, approximately 60% of PMD patients have duplications of the *PLP* gene (Sistermans et al. 1998; Woodward et al., 1998; Inoue et al., 1999). Thus, abnormality in the quantity of *PLP* gene also leads to PMD/SPG2.

Studies in our laboratory, together with others, previously showed that PLP-overexpressing mice undergo oligodendrocyte cell death and demyelination at rates depending on expressed gene dosage (Kagawa et al., 1994; Readhead et al., 1994). In our "4e" line, homozygous transgenic (*Plp/Plp*) mice with four extra copies of *Plp* gene exhibit severe hypomyelination, tremors, and convulsions, and die by 4 weeks of age. In contrast, heterozygous (*Plp/-*) mice that express approximately 30% more *PLP* transcripts, myelinate normally such that young (<3months old) animals have ultrastructurally normal-appearing myelin. By 3 months of age, however, they begin to show signs of degeneration of myelin, and by 7 months of age, axons are fully demyelinated (Kagawa et al., 1994; Inoue et al., 1996). These *Plp/-* mice are the only available animal model for spontaneous late-onset chronic demyelination.

Molecular events involved in this demyelination process are poorly understood. Especially it is totally unknown why the oligodendrocytes cannot remyelinate the naked axons at the later stages of development, while they were capable of forming normal myelin at an early stage. Lack of remyelination in active demyelinating lesions is a problem in other demyelinating diseases as well, including multiple sclerosis (MS). In the MS patients initial degeneration of myelin membrane involves immunological reaction, while the myelin membrane spontaneously degenerates in our *Plp/-* mice, thus the trigger of demyelination is

different between MS and *Plp/-* mice. However, in both cases remyelination is always observed and it is only when active remyelination is disrupted, the axons become naked resulting in appearance of severe symptoms.

Thus I aimed to characterize the molecular events involved in the demyelinating process in the *Plp/-* mice. I carefully reexamined the demyelinating process and found that remyelination is severely affected at an old age, accompanied by invasion of many cells into the lesion sites. I showed the presence of oligodendrocyte progenitors (OLPs) in demyelinating area of the *Plp/-* mice, thus OLP-deprivation is not the cause of inefficient remyelination. On the other hand the microenvironment was shown to be inhibitory to OLP differentiation/maturation through the transplantation experiment. This change was at least partially caused by the upregulation of PSA-NCAM and cystatin C. Next, I obtained morphological and molecular evidence of astrocyte-, microglia-activation by immunohistochemistry and in situ hybridization using various markers. My results demonstrate that astrocytes and microglias are activated from an early time course of demyelination, even before any signs of abnormal behaviour is observed. These abnormalities may be responsible for the inhibition of remyelination.

Experimental procedures

Materials:

In this study, I used PLP overexpressing transgenic mice, 4e line (Kagawa et al., 1994). These transgenic mice were backcrossed to BDF1 (SLC Inc., Tokyo, Japan). All animal procedures were conducted in accordance with guidelines described by the National Institutes of Health Guide for Care and Use of Laboratory Animals and the local Animal Care and Use Committee.

PBS (cat, #21600-051), Dulbecco's modified eagle's medium (DMEM)/F12 (cat#12400-024), transferrin (cat #11108-016) and insulin (cat #18125-039) were purchased from Invitrogen (CA, USA). DNase I (cat #1-284-932) was purchased from Roche (Basel, Switzerland). Trypsin inhibitor (cat #T-9003), progesterone (cat #P-6149), sodium selenate (cat #S-5779) and putrescine (cat #P-7505) were purchased from SIGMA (MO, USA). EGF (human recombinant) (cat #100-15) and bFGF (human recombinant) (cat #100-18B) were purchased from Pepro Tech EC (London, UK). Six well ultra-low cluster plates (cat #3471; costar) were purchased from Corning (NY, USA) and Charcoal (cat #038-02145) was purchased from Wako Pure Chemical Industries (Osaka, Japan).

Monoclonal anti-PSA-NCAM antibody 12E3 (Seki et al., 1991) was a gift from Dr.

Seki in the Juntendo University School of Medicine (Tokyo, Japan). Polyclonal anti-MBP antibody (cat, #L1829) and polyclonal anti-GFAP antibody (cat #Z0334) was purchased from DAKO (Glostrup, Denmark). Monoclonal anti-MBP antibody (cat #1118009) was purchased from Boehringer Mannheim (Mannheim, Germany). Polyclonal anti-GFP antibody (cat #A-6455) was purchased from Molecular Probes (OR, USA). Biotin conjugated anti-mouse IgM antibody (mu-chain specific; cat #BA-2020), biotin conjugated anti-rabbit IgG antibody (cat #BA-1000) and ABC Elite Standard Kit^{TM} (cat #PK-6100) were purchased from Vector Laboratories (CA, USA). Secondary fluorescent antibodies, Alexa Fluor 594 goat anti-mouse IgG (H+L) (cat #A-11032) and Alexa Fluor 488 goat anti-rabbit IgG (H+L) (cat #A-11008) were purchased from Molecular Probes (OR, USA). APS-coated glass slides (cat #S-8226) were purchased from Matsunami (Osaka, Japan).

Taq polymerase for RT-PCR (cat #M1661) was purchased from Promega (WI, USA). DIG RNA labeling kit (cat #1175025) and RNase free DNase (cat #1119915) were purchased from Roche. Trizol (cat # 15596-018) and Superscript II (cat #18064-022) were purchased from Invitrogen (CA, USA). ExTaq DNA polymerase (cat #RR001A) was purchased from Takara Bio (Shiga, Japan). AmpliTaq Gold DNA Polymerase (cat #N808-0244) for genotyping was purchased from Applied Biosystems (CA, USA).

General reagents were purchased from Wako Pure Chemical Industries.

Procedures:

Genotyping the PLP transgenic mice

For genotyping, I used a methods previously described with minor modifications (Kagawa et al., 1994). Genomic DNA was extracted and Taq polymerase primers (4e'2 primer, 5'-CAA TGC GCT TAC TGA TGC GG-3'; 4e'3 primer 5'- CGC ACA GAA GCT ATT ATG CG-3'; Crx-F2, 5'-TAC TCA AGT GCC CCT AGG AAG C-3'; Crx-R2, 5'-ATT GAT CTT AAG AGC AAC CTC C-3') which amplify 258 bp fragment from 3'-arm of cosmid vector, Lorist B and 138 bp fragment from *Crx* gene (GenBank accession number: NT_039395). PCR was carried out with AmpliTaq Gold DNA Polymerase for 32 cycles as follows: 95℃ for 20 sec, 56℃ for 30 sec, and 72℃ for 30 sec. PCR products were separated by electrophoresis on 2% agarose gel and stained with ethidium bromide.

Tissue Preparation

Cryosections

Brain: The mice were deeply anesthetized with sodium pentobarbital, and perfused intracardially first with 0.01 M PBS, pH 7.4, followed by 4% paraformaldehyde (PFA) in

0.1 M PB, pH 7.4. The brains were removed from the skull, immersed in 10% sucrose for 2-3 hr, then in 20% sucrose in PBS at 4℃ overnight, embedded in O.C.T. Compound (Sakura Finetechnical Co., cat #4583) and stored at –80℃. The brains were sectioned at 18 or 20 μm thickness using a cryostat (Leica, CM3050S) for ISH or immunohistochemistry.

Brain (transplanted): The mice were deeply anesthetized with sodium pentobarbital, and perfused with 1.0% PFA in 0.1 M PB, pH 7.4 at 20 days post-transplantation. Brains were collected, post fixed, cryoprotected, and frozen. Sagittal and coronal cryosections (30 μm thickness) were processed for double immunohistochemistry.

Paraffin sections

After perfusion, the brains were removed from the skull and placed in the same fixative overnight at 4℃. The brains were dehydrated through a graded ethanol series and embedded in paraffin. The tissues were then sectioned at 6 μm thickness.

Semi-ultrathin sections

Semi-ultrathin sections were prepared by a method previously described. (Ding et al., 2002).

Immunohistochemistry

PSA-NCAM staining

Cryosections (20 μm thickness) were washed in PBS. For removal of lipid, sections were dehydrated through a graded ethanol series, treated with xylene for 30 min, and then rehydrated. Sections were treated with 0.05% H_2O_2 in PBS for 30 min, washed with PBS, and treated for 1 hr with blocking buffer (PBS with 1% normal goat serum) followed by overnight incubation at 4℃ with primary antibody (dilutions: 12E3, 1/500) which was diluted in the blocking buffer. Sections were washed with PBS, incubated for 1 hr at room temperature in biotin conjugated anti-mouse IgM antibody (dilutions: 1/200) which was diluted in PBS. Sections were washed with PBS and incubated with AB complex (ABC Elite Standard Kit™) at room temperature for 1 hr. Sections were washed with PBS, stained with the solution containing 0.5 μg/ml DAB and 0.015% H_2O_2 in PBS under a microscope and the reaction was stopped with water. The image was collected by Olympus digital camera system (DP70) using microscopy (Olympus BX51).

GFAP staining

Cryosections (20 μm thickness) were washed in PBST (PBS containing 0.1% Triton-X100). Sections were treated with 0.05% H_2O_2 in PBST for 30 min, washed with PBST, and treated for 1 hr with blocking buffer (PBST with 10% normal goat serum)

followed by overnight incubation at 4℃ with polyclonal anti-GFAP antibody (dilutions: 1/2000) which were diluted in the blocking buffer. Sections were washed with PBST, incubated for 1 hr at room temperature in biotin conjugated anti-rabbit IgG antibody (dilutions: 1/200) which was diluted in PBST. Sections were washed with PBST and incubated with AB complex (ABC Elite Standard Kit™) at room temperature for 1 hr. Sections were washed with PBST, stained with the solution containing 0.5 μg/ml DAB and 0.015% H_2O_2 in PBS under a microscope and the reaction was stopped with water.

MBP staining

After deparaffinization and rehydration, paraffin sections were treated with 0.05% H_2O_2 in PBST for 30 min, washed with PBST, and treated for 1 hr with blocking buffer (PBST with 1% normal goat serum) followed by overnight incubation at 4℃ with polyclonal anti-MBP antibody (dilutions: 1/2) which were diluted in the blocking buffer. Sections were washed with PBST, incubated for 1 hr at room temperature in biotin conjugated anti-rabbit IgG antibody (dilutions: 1/200) which was diluted in PBST. Sections were washed with PBST and incubated with AB complex (ABC Elite Standard Kit™) at room temperature for 1 hr. Sections were washed with PBST, stained with the solution containing 0.5 μg/ml DAB and 0.015% H_2O_2 in PBS under a microscope and the

reaction was stopped with water. The sections were then counterstained by the Nissl method (0.1% cresyl violet).

Immunofluorescence double labeling

Cryosections (30 µm thickness) were rehydrated for 5 minutes in PBS. The primary antibodies were diluted in PBST with 10% goat serum (mouse monoclonal anti-MBP antibody at 1:500 dilution, rabbit polyclonal anti-GFP antibody at 1:5000 dilution) and applied for overnight at 4℃. Sections were then rinsed three times with PBST and incubated for 30 minutes at room temperature with fluorescent secondary antibodies, Alexa Fluor 594 goat anti-mouse IgG (H+L) and Alexa Fluor 488 goat anti-rabbit IgG (H+L), diluted in PBST (dilutions: 1/1000). After three washes in PBST, sections were coverslipped and observed with a fluorescence microscope.

Histology

Hematoxylin and eosin staining and Kluver-Barrera's staining using LFB and cresyl violet were performed on paraffin sections in accordance to conventional methods. Counter staining with methyl green or cresyl violet were performed in accordance to conventional methods.

In situ hybridization

For in situ hybridization on cryosections (18 μm thickness), I used a modification of methods previously described (Wilkinson, 1992). After in situ hybridization staining, the sections were counterstained by nuclear fast red. For generating probes, the following plasmids containing mouse cDNA: *Olig1*, *Olig2* (Takebayashi et al., 2000), and *cystatin C* (GenBank accession number: NM_009976, 21-636bp in pBluescript II SK(-) vector) were used. Following plasmids were obtained from Invitrogen as mouse EST clones: *Sox10* (GenBank: BF535140), *c-fms* (GenBank: AA473814), and *DAP12* (GenBank: AA734769). Digoxigenin-labeled single-stranded riboprobes were prepared by transcription of linearized plasmids using T7, T3 or Sp6 RNA polymerase and DIG RNA labeling kit.

Quantification of STX and PST mRNAs by RT-PCR

Total RNA from mouse retina was isolated using Trizol according to the manufacturer's instructions and treated with RNase free DNase (0.02 U/ml). Total RNA (5 μg) was used to generate cDNA by Superscript II in a total volume of 20 μl with oligo-dT primers. The RT-PCR primers for *α2,8polysialyltransferase type IV* (*ST8SiaIV*; *PST*) and *α2,8polysialyltransferase type II* (*ST8SiaII*; *STX*) were reported previously (Soares et al., 2000). PCR was performed with ExTaq DNA polymerase. After an initial step of 3

min at 94°C, the reaction was run for 35 cycles with 30 sec at 94°C, 30 sec at 58°C for *STX* and 62°C for *PST*, then 1 min at 72°C. Amplified products (528 bp for *STX* and 606 bp for *PST*) were checked by 1% agarose gel electrophoresis. To normalize among the sample variation, the level of *glyceraldehyde-3-phosphate dehydrogenase* (*GAPDH*) mRNA was also measured as an internal control at 20 cycles of RT-PCR using following primers (5'-ATG GTG AAG GTC GGT GTG AAC GGA-3', 5'-TTA CTC CTT GGA GGC CAT GTA GGC-3') which amplifies 1004 bp-fragment.

Quantitative analysis of cell numbers on tissue sections

Total cell number in corpus callosum

Number of total cells was determined per square unit of tissue in corpus callosum. The number of nuclei stained by cresyl violet was counted in 5 standardized 22,500μm^2 (150μm×150μm) microscopic fields per section (6 μm thickness), each defined by ocular morphometric grid. Two sections of one mouse per condition were analyzed.

Olig1+ cell number in corpus callosum

The number of cells expressing *Olig1* mRNA was determined per image of tissue in corpus callosum. The number of stained cells was counted for 5 captured images of

60,366 μm^2 (282.84μm×213.43μm) each per section (18 μm thickness). Two sections per mouse were analyzed. Two mice per condition were used.

GFAP+ cell number in cortex

The number of GFAP+ cells was determined per field of view of tissue in cortex. The number of GFAP+ cells with nuclei stained by cresyl violet was counted for 2 fields of 330,000μm^2 (circle with a diameter of 0.65mm) each per section (20 μm thickness). Two sections per mouse were analyzed. Two mice per condition were used.

Neurosphere culture

Donor cells were obtained from green mice expressing EGFP in all the somatic cells (Shibasaki et al., *in press*) at embryonic day 14.5. The day of vaginal plug detection was considered 0.5 days post coitum. Green mouse fetuses were removed from the uterus of timed pregnant mice. The fetuses were placed in Petri dishes containing 10-12 ml of PBS at room temperature. After three times washing, each telencephalon was separated into two cerebral hemispheres. After removing pia mater, ganglionic eminences were dissected out from the hemispheres. The tissues were minced and treated with 0.25% trypsin and 0.05% DNase I in PBS for 13 min at 37˚C. The digestion was terminated with

trypsin inhibitor. The sections were dissociated by gentle pipetting with a fire-polished Pasteur pipette, and incubated for 1 min. Upper 80% v/v of the cell suspension was transferred to a new tube to remove the non-dissociated cell blocks. DNase I (final 0.05%) was added to the cell suspension followed by centrifugation at 800 rpm for 10 min. After removing the supernatant, cells were resuspended in the Dulbecco's modified eagle's medium (DMEM)/F12 containing 0.6% glucose, 14 mM sodium bicarbonate, 100 μg/ml transferrin, 25 μg/ml insulin, 20 nM progesterone, 30 nM sodium selenate, 60 μM putrescine, 20 ng/ml EGF (human recombinant) and 20nM bFGF (human recombinant), plated at 9.6×10^4 cells/3ml medium in each well of a 6 well ultra-low cluster plate, and then incubated at 37˚C in a humidified atmosphere of 5% CO_2. Primary spheres were collected at 8 day in vitro (DIV). They were then triturated, spun down, resuspended, and plated at 4.8×10^4 cells/3ml medium in each well of the 6 well plate. Secondary spheres were collected at 4 DIV. The day of the cells were plated was defined as 0 DIV.

Transplantation

Eight months PLP-4eTg mice were deeply anesthetized (intraperitoneal injection of xylazine, 10mg/kg and ketamine, 100mg/kg), fixed with stereotaxic apparatus (Narishige, SR-5N; Tokyo, Japan) and incised at approximately 1.5 mm to the left of the skull midline

and 1.5 mm rostral to the bregma. A drawn glass micropipette connected to a 10µl Hamilton syringe held by infusion syringe pumps (Stoelting Co., model 310; IL, USA) was introduced at 2.4 mm deep from the skull surface of the bregma and 2 µl of culture medium containing secondary spheres were injected (flow rate, 0.4µl/min). Charcoal was attached to the tip of the micropipette before transplantation in order to confirm the site of transplanted graft.

Results

Late-onset progressive demyelination and lack of myelin-regeneration in aged PLP-overexpressing transgenic mice

I first confirmed late-onset demyelination in the optic nerve of *Plp/-* mice. Semi-ultrathin sections from 1 month old mouse optic nerves were examined under optic microscope. Myelin formation proceeded normally in the *Plp/-* mice and there was little difference in the appearance of myelin membrane between the wild type and *Plp/-* mice (Fig. 1A, B). At 6 months of age the myelin structure was mostly intact (Fig. 1C) although electron micrographic analysis indicated the presence of degenerated myelin membrane in the 6 months old *Plp/-* mice optic nerve (Inoue et al., 1996). Demyelination abruptly proceeded by 7 months of age in the optic nerve of *Plp/-* mice (Fig. 1D), however, there were signs of remyelination as indicated by the thin myelin membrane (Arrows in Fig 1D), which is consistent with the observation by Inoue et al. (1996). At 8 months of age all the axons in the *Plp/-* mice optic nerves became naked without any signs of remyelination (Fig. 1E). Thus the severe demyelinating phenotype is at least partially caused by the lack of remyelination in this mouse.

There are three possible causes for the lack of remyelination after aging. One is the lack of oligodendrocyte progenitor (OLP) pool by vigorous consumption. Second possibility is that the OLPs of the *Plp/-* mice intrinsically loose their ability to mature after certain age. The last possibility is the change of microenvironment into that inhibiting differentiation/maturation of oligodendrocyte. To examine these possibilities I focused on the corpus callosum because it is easy to transplant cells into this structure. Thus I first confirmed the time course of demyelination in the corpus callosum by Kluver-Barrera's staining at various stages (2, 4 and 8 months).

I did not observe any obvious change of myelin stained by luxol fast blue (LFB) at 2 months (Fig. 2B, C) and 4 months (Fig. 2D, E), however, massive demyelination was observed in the *Plp/-* mice, in contrast to wild mice at 8 months (Fig. 2F, G). These observations were consistent with our previous ultrastructural analysis of cerebellum and spinal cord (Kagawa et al., 1994). The demyelination was also confirmed by immunohistochemical analysis using anti-myelin basic protein (MBP) antibody (Fig. 4A-D). As demyelination progressed, there were many accumulating cells in the corpus callosum of the *Plp/-* mice (Fig. 4A-B). With high magnification image of hematoxylin and eosin (HE) staining (Fig. 4E, F), most of them had small and dense nuclei and scarce cytoplasm.

The number of the cells in the white matter was counted (Fig. 3). At 8 months of age when the region was totally demyelinated there was a great increase in the number of cells in corpus callosum (2036±352 [mean±SD] cells/ mm^2 in wild type and 5196±1495 in *Plp/-* mice at 8 months; 2 sections from 1 brain; Fig. 3).

Oligodendrocyte progenitors are present in chronic demyelinating legions

I first analyzed whether the number of OLPs is reduced when active demyelination is occurring using recently identified markers, Olig1, Olig2 (Lu et al., 2000; Takebayashi et al., 2000; Zhou et al., 2000) and Sox10 (Kuhlbrodt et al. 1998; Zhou et al., 2000). *Olig1* positive OLPs were present all over the CNS in *Plp/-* mice, including the demyelinated lesions (Fig. 5). In wild type mice, the number of *Olig1* positive-OLPs decreased gradually (Fig. 5A, C, E), while, accumulation of *Olig1* positive-OLPs were observed in the demyelinating corpus callosum (362±141 [mean±SD] *Olig1*$^+$ cells/ mm^2 in wild type and 890±371 in *Plp/-* mice at 8 months; 4 sections from 2 brain). Similar data were also obtained using ISH probes for *Olig2* (data not shown) and *Sox10* (Fig. 6). Furthermore, I also confirmed that OLPs were present even in the 15 months old *Plp/-* brain by the same ISH probes (data not shown). These data suggest that OLPs are present in the CNS of *Plp/-* mice throughout the life and are recruited to the demyelinating legion. Since OLPs in the *Plp/-* mice are able to form myelin in the early life,

they might fail to differentiate into remyelinating oligodendrocyte due to an intrinsic character of the OLPs in the aged *Plp/-* mice (2nd possibility) or to an inhibitory microenvironment in the late life (3rd possibility).

Very little oligodendrocytes were generated from the transplanted neurosphere.

To understand which possibility is the main cause for the late onset demyelination the transplantation experiment was performed. Neurospheres were prepared from E14.5 ganglionic eminence of transgenic mice expressing EGFP under control of CAG promoter, which is strongly active in all cells in the transgenic mouse (Shibasaki et al., *in press*). The neurospheres were transplanted into the corpus callosum of 8 months old *Plp/-* mice. Twenty days after transplantation, grafted cells remained at the vicinity of the injection site. This was in contrast to the result of experiments in which *shiverer* mice were used as a host (Vitry et al., 2001). Some grafted cells differentiated into oligodendrocyte and seemed to myelinate axons, but most of the cells seemed to differentiate into astrocyte (Fig.7).

This result indicates that the environment in the *Plp/-* mouse brain is inhibitory to oligodendrocyte differentiation/maturation and caused massive demyelination due to the inhibition of remyelination at a late stage.

Inhibitory molecule against myelination is up-regulated at chronic phase of demyelination

I first looked for the changes on the axonal surface that would account for inhibition of remyelination. As one candidate, I focused on PSA-NCAM, because PSA-NCAM is reported to be a potential inhibitor of myelination (Charles et al., 2000; Charles et al., 2002). I stained 4, 8 and 10 months old wild type and *Plp/-* mouse corpus callosum with anti-PSA-NCAM antibody and their adjacent sections with anti-MBP antibody. At 4 months of age, when demyelination is not obvious, there was no staining of PSA-NCAM in both animals (Fig. 8A-D). However, there was up-regulation of PSA-NCAM immunoreactivity in the corpus callosum of 10 months old *Plp/-* mouse (Fig. 8G). At a higher power image, it is suggested that PSA-NCAM is up-regulated in reactive astrocytes (Fig. 8I). At coronal sections from 8 months old animal it is much clearer that PSA-NCAM is also up-regulated on the axonal surface (Fig. 9A-E). In order to confirm that the up-regulation of PSA-NCAM occurred in axon, I performed RT-PCR analyses of synthetic enzymes, *STX* and *PST* using retinal mRNA. Since there are no oligodendrocytes in rodent retina and retinal ganglion cells extend axons from soma in retina into optic nerve where demyelination occurs, I can detect neuronal response against demyelination on axons by using retinal mRNA. The data shows that *PST* mRNA is up-

regulated by 5 months of age (Fig. 10). *STX* expression was not detectable (data not shown), which was consistent to the previous report that *PST* is the major synthetic enzyme at an adult stage (Hildebrandt et al., 1998).

We have also shown that cystatin C, a cysteine protease inhibitor, is inhibitory against oligodendrocyte development (Hasegawa et al., in preparation). Thus I studied cystatin C expression in the brain of *Plp/-* mouse. I performed in situ hybridization (ISH) using probe for *cystatin C*. Up-regulation of cystatin C was reported in the brain under various pathological conditions (Aronica et al., 2001; Steinhoff et al., 2001) including MS lesion (Chabas et al., 2001) and it was suggested that production of cystatin C is up-regulated in reactive astrocytes and microglia (Aronica et al., 2001). Increasing number of cystatin C producing cells was observed at all the age observed (Fig. 11A-F). I also confirmed that most of cystatin C-producing cells are astrocytes by combination of *cystatin C* ISH and GFAP immunostaining (Fig. 11G).

These results clearly showed that PSA-NCAM and cystatin C is overexpressed in the *Plp/-* mouse brain, and are, at least partially, responsible for the inhibition of oligodendrocyte development.

Response of astrocyte during demyelination

Since these factors are mainly produced by astrocytes, I next focused on astrocytes. It is also reported that reactive astrocytes play important roles in demyelination in multiple sclerosis (MS) (John et al., 2002), or in experimental autoimmune encephalomyelitis (EAE) (Van Der Voorn et al., 1999; Fife et al., 2000; Izikson et al., 2000). I performed immunohistochemical analysis of 2, 4 and 10 months old wild type and *Plp/-* mice using anti-glial fibrillary acidic protein (GFAP) antibody. GFAP-immunostaining was stronger in the *Plp/-* mice than in wild type animals at all the ages studied (Fig. 12A-F). At higher magnification the morphology of astrocytes appeared hypertrophic with increased process thickness, all of which are characteristics of reactive astrocytes (Fig.12G, H). I also observed increase in the number of GFAP-expressing cells (126±23 [mean±SD] $GFAP^+$ cells/ mm^2 in wild type and 327±60 in *Plp/-* mice at 2 months; 2 sections from 2 brains; Fig. 13). Interestingly the change in astrocyte morphology and number were observed from 2 months of age, indicating that activation of astrocyte occurs much earlier than when demyelination become obvious.

Microglial activation precedes demyelination

Since activated microglias were detected by the electron micrography in the optic nerve of *Plp/-* mouse (Inoue et al., 1996), I next studied the change in the number and activation of microglia during the course of demyelination. For ISH detection of microglia/brain macrophage distribution and activation, I used two markers, c-fms and DAP12. c-Fms is a tyrosine receptor for macrophage colony stimulating factor (M-CSF), expressed in microglia in the CNS (Raivich et al., 1991) and DAP12 is a transmembrane adaptor, well known for its role in transducing activation signals for an extended array of receptors in NK cells, granulocytes, monocytes/macrophages (Lanier and Bakker., 2000). DAP12 expression was reported to be elevated in activated microglia by microarray analysis (Ohmi et al., 2003). By *c-fms* ISH, I observed that *c-fms* expression become weaker as the mice age (corpus callosum and hippocampus; Fig. 14A, C, E, cerebellum; Fig. 15A, C, E). However, in the *PLP/-* brain its expression level does not decrease and as a result there is a big difference in the expression level and the number of cells expressing *c-fms* between the wild type and *PLP/-* mouse by 8 months (corpus callosum and hippocampus; Fig. 14B, D, F, cerebellum; Fig. 15B, D, F).

There were no *DAP12* positive cells in wild type brains (corpus callosum and hippocampus; Fig. 16A, C, E, cerebellum; Fig. 17A, C, E). On the other hand there were many *DAP12* positive cells in *PLP/-* brains (corpus callosum and hippocampus; Fig. 16B, D, F,

cerebellum; Fig. 17 B, D, F). Interestingly, I detected many DAP12 positive cells in the white matter of *PLP/-* brain already at 2 months of age (Fig. 16B), long before the active demyelination occurs in this region. At 8 months of age its expression became much stronger (Fig. 16F), suggesting strong activation of microglia at an active demyelinating stage.

Taken together, these data indicate that microglia are activated much earlier than demyelination become obvious and imply that they have important role in an early as well as late phase of demyelination.

Discussion

In this study, I analyzed neuropathology of unique demyelinating mouse model overexpressing the *PLP* gene. One of the major findings in this study is the lack of remyelination in the aged (8 months old) *Plp/-* mice (Fig. 1). This was accompanied by the total loss of myelin in the optic nerve and a massive cell infiltration. I focused on understanding the mechanisms that inhibit remyelination in the aged animals. First I checked whether it is caused by the deprivation of OLPs. However, in situ hybridization studies using *Olig1*, *Olig2* or *Sox10* probes showed that there are more OLPs in the demyelinated lesions (Fig. 5, 6) than in corresponding regions of the wild type animals. Therefore, differentiation/maturation of OLPs were inhibited in the brains of aged *Plp/-* mouse. To distinguish whether this is caused by the intrinsic properties of the aged *Plp/-* mouse OLPs or by the environmental effect, I transplanted neurospheres containing neural stem cells and possibly OLPs into the demyelinated corpus callosum. The results demonstrated that the transplanted cells poorly developed into myelinating oligodendrocytes. A similar procedure has been taken to treat dysmyelinating mice, such as the *shiverer* mouse. In this case the transplanted cells migrated and distributed in a wide area of the brain, and efficiently developed into myelinating

oligodendrocytes (Vitry et al., 2001). Thus I concluded that the environment of the aged *Plp/-* mouse brain is inhibitory for the differentiation/maturation of OLPs.

I next studied what is the cause for this environmental change. It is known that axonal properties change during demyelination, for example, sodium channel clustering (Ishibashi et al., 2003), dysregulation of sodium channel isoforms (Rasband et al., 2003), and axonal degeneration (Anderson et al., 1998). In this study, I demonstrated upregulation of PSA-NCAM in axons and also in astrocytes. This molecule is known to inhibit maturation of OLPs in vitro and is present in unmyelinated axons, but disappears when myelination starts. PSA-NCAM is also upregulated in the demyelinated lesions of multiple sclerosis patients. It is possible that axons that have been exposed to a sustained active glial environment might become damaged to such an extent that they no longer express the appropriate signals to be remyelinated.

I also found that cystatin C expression is upregulated in the demyelinated lesion. Cystatin C is a cysteine protease inhibitor, but has also been reported to be a cofactor of FGF2 and functions in maintaining the neural stem cells in a proliferating stage, independent of its protease inhibitory activity (Taupin et al., 2000). Hasegawa in our laboratory has found that cystatin C stimulates differentiation of astrocyte while inhibiting that of oligodendrocytes (manuscript in preparation). Thus upregulation of cystatin C is also inhibitory for

oligodendrocyte development. I was not able to obtain clear data from cystatin C immunohistochemical analysis, probably because it is abundantly secreted into the extracellular space and secreted cystatin C is incorporated into other cells (Merz et al., 1997). The role of cystatin C upregulation in pathological condition remains unclear. Some role is expected by inhibiting proteases, such as cathepsins (Aronica et al., 2001), but other roles may be related to be the modulation of differentiation of glial cells.

The change in the expression levels of PSA-NCAM and cystatin C, that are expressed in non-oligodendroglial cells, and a massive infiltration of the cells in the demyelinated lesions prompted me to study cell types present in the demyelinating brain.

Morphological change of astrocyte into reactive astrocyte-like shape and increase in the number was observed as early as 2 months of age. At this stage there are no observable abnormality in the myelin structure nor in their behavior (Kagawa et al., 1994; Inoue et al., 1996). The number of GFAP positive cells in the *Plp/-* mouse brain did not increase with aging or with the progress of demyelination. Thus astrocytes detect very early sign of demyelination and become activated. I should investigate whether this activation is further stimulating the demyelination process or suppressing it.

Many lines of evidences suggest that the activation of macrophage/microglia in MS lesions plays central role in the effector phase of myelin breakdown (Cua et al., 2003). Since little was known about microglial responses during demyelination in the *Plp/-* mice, I investigated it using microglial markers, c-fms and DAP12. Since DAP12 expression level was elevated in activated microglia detected by the microarray analysis (Ohmi et al., 2003), I used DAP12 as an ISH marker for activated microglia in this study. As expected, DAP12 was expressed in activated microglia and allowed me to visualize active demyelinating lesions with high sensitivity from an early stage. So far, we have no evidence of inflammation (unpublished data; Anderson et al., 1998). Collectively, my data suggest that during demyelination, resident microglial cells and astrocytes becomes activated, astrogliosis occurs, and these cells may change the environment to that inhibitory for oligodendrocyte differentiation/maturation. I have shown that these glial cells express PSA-NCAM and cystatin C, but they should also be secreting many other cytokines as well, that may be inhibiting remyelination.

Primary cause of demyelination in the *Plp/-* mice is PLP-overexpression in oligodendrocyte. My analyses suggest that abnormal responses occur in other cell types than oligodendrocytes and that combination of cell intrinsic mechanisms (Southwood and Gow, 2001; Simons et al., 2002) and cell extrinsic mechanisms (this study) lead to defective re-myelination in the mice.

Furthermore, my result suggests that glial cells are responding to a very early sign of demyelination and this could be used for early detection of demyelination. Notch ligand, Jagged has been shown to be expressed in the astrocytes of MS patients, which is inhibitory for oligodendrocyte maturation (John et al., 2002). I showed that PSA-NCAM is expressed by the astrocytes as well as in the axon. Moreover, I showed cystatin C is expressed by the astrocytes. It is important to study whether these two molecules I found to be expressed in glial cells during demyelination, have some role during progression of human demyelinating disease. Further investigation is required to understand the molecular mechanisms of demyelination and to establish therapeutic intervention. My study shows one direction into which we should proceed to solve these problems.

Acknowledgements

I would like to express my sincere appreciation to Professor Kazuhiro Ikenaka, Dr Hirohide Takebayashi and Dr. Tetsushi Kagawa for their generous support and valuable guidance throughout this study. I would like to thank Dr. Tatsunori Seki (Juntendo University) for providing anti-PSA-NCAM antibody 12E3. I thank François Lachapelle (INSERM, France) for teaching me transplantation. I am grateful to all members of Ikenaka laboratory, especially Rie Taguchi for help in genotyping, Daisuke Nakamura for assistance of in situ hybridization, and Drs. Fujimoto Ichiro, Katsuhiko Ono and Seiji Hitoshi for helpful discussion.

References

Anderson TJ, Schneider A, Barrie JA, Klugmann M, McCulloch MC, Kirkham D, Kyriakides E, Nave KA, Griffiths IR: Late-onset neurodegeneration in mice with increased dosage of the proteolipid protein gene. J Comp Neurol 1998; 394: 506-519.

Aronica E, van Vliet EA, Hendriksen E, Troost D, Lopes da Silva FH, Gorter JA: Cystatin C, a cysteine protease inhibitor, is persistently up-regulated in neurons and glia in a rat model for mesial temporal lobe epilepsy. Eur J Neurosci 2001; 14: 1485-1491.

Chabas D, Baranzini SE, Mitchell D, Bernard CC, Rittling SR, Denhardt DT, Sobel RA, Lock C, Karpuj M, Pedotti R, Heller R, Oksenberg JR, Steinman L: The influence of the proinflammatory cytokine, osteopontin, on autoimmune demyelinating disease. Science 2001; 294: 1731-1735.

Charles P, Hernandez MP, Stankoff B, Aigrot MS, Colin C, Rougon G, Zalc B, Lubetzki C: Negative regulation of central nervous system myelination by polysialylated-neural cell adhesion molecule. Proc Natl Acad Sci U S A 2000; 97: 7585-7590.

Charles P, Reynolds R, Seilhean D, Rougon G, Aigrot MS, Niezgoda A, Zalc B, Lubetzki C: Re-expression of PSA-NCAM by demyelinated axons: an inhibitor of remyelination in multiple sclerosis? Brain 2002; 125: 1972-1979.

Cua DJ, Sherlock J, Chen Y, Murphy CA, Joyce B, Seymour B, Lucian L, To W, Kwan S, Churakova T, Zurawski S, Wiekowski M, Lira SA, Gorman D, Kastelein RA, Sedgwick JD: Interleukin-23 rather than interleukin-12 is the critical cytokine for autoimmune inflammation of the brain. Nature 2003; 421: 744-748.

Ding L, Yamada K, Takayama C, Inoue Y: Development of astrocytes in the lamina cribrosa sclerae of the mouse optic nerve, with special reference to myelin formation. Okajimas Folia Anat Jpn 2002; 79: 143-157.

Fife BT, Huffnagle GB, Kuziel WA, Karpus WJ: CC chemokine receptor 2 is critical for induction of experimental autoimmune encephalomyelitis. J Exp Med 2000; 192: 899-905.

Griffiths I, Klugmann M, Anderson T, Thomson C, Vouyiouklis D, Nave KA: Current concepts of PLP and its role in the nervous system. Microsc Res Tech 1998; 41: 344-358.

Hildebrandt H, Becker C, Murau M, Gerardy-Schahn R, Rahmann H: Heterogeneous expression of the polysialyltransferases ST8Sia II and ST8Sia IV during postnatal rat brain development. J Neurochem 1998; 71: 2339-2348.

Hodes ME, Pratt VM, Dlouhy SR: Genetics of Pelizaeus-Merzbacher disease. Dev Neurosci 1993; 15: 383-394.

Inoue K, Osaka H, Imaizumi K, Nezu A, Takanashi J, Arii J, Murayama K, Ono J, Kikawa Y, Mito T, Shaffer LG, Lupski JR: Proteolipid protein gene duplications

causing Pelizaeus-Merzbacher disease: molecular mechanism and phenotypic manifestations. Ann Neurol 1999; 45: 624-632.

Inoue Y, Kagawa T, Matsumura Y, Ikenaka K, Mikoshiba K: Cell death of oligodendrocytes or demyelination induced by overexpression of proteolipid protein depending on expressed gene dosage. Neurosci Res 1996; 25: 161-172.

Ishibashi T, Ikenaka K, Shimizu T, Kagawa T, Baba H: Initiation of sodium channel clustering at the node of Ranvier in the mouse optic nerve. Neurochem Res 2003; 28: 117-125.

Izikson L, Klein RS, Charo IF, Weiner HL, Luster AD: Resistance to experimental autoimmune encephalomyelitis in mice lacking the CC chemokine receptor (CCR)2. J Exp Med 2000; 192: 1075-1080.

John GR, Shankar SL, Shafit-Zagardo B, Massimi A, Lee SC, Raine CS, Brosnan CF: Multiple sclerosis: re-expression of a developmental pathway that restricts oligodendrocyte maturation. Nat Med 2002; 8: 1115-1121.

Kagawa T, Ikenaka K, Inoue Y, Kuriyama S, Tsujii T, Nakao J, Nakajima K, Aruga J, Okano H, Mikoshiba K: Glial cell degeneration and hypomyelination caused by overexpression of myelin proteolipid protein gene. Neuron 1994; 13: 427-442.

Kuhlbrodt K, Herbarth B, Sock E, Hermans-Borgmeyer I, Wegner M: Sox10, a novel transcriptional modulator in glial cells. J Neurosci 1998; 18: 237-250.

Lanier LL, Bakker AB: The ITAM-bearing transmembrane adaptor DAP12 in lymphoid and myeloid cell function. Immunol Today 2000; 21: 611-614.

Lu QR, Yuk D, Alberta JA, Zhu Z, Pawlitzky I, Chan J, McMahon AP, Stiles CD, Rowitch DH: Sonic hedgehog--regulated oligodendrocyte lineage genes encoding bHLH proteins in the mammalian central nervous system. Neuron 2000; 25: 317-329.

Merz GS, Benedikz E, Schwenk V, Johansen TE, Vogel LK, Rushbrook JI, Wisniewski HM: Human cystatin C forms an inactive dimer during intracellular trafficking in transfected CHO cells. J Cell Physiol 1997; 173: 423-432.

Ohmi K, Greenberg DS, Rajavel KS, Ryazantsev S, Li HH, Neufeld EF: Activated microglia in cortex of mouse models of mucopolysaccharidoses I and IIIB. Proc Natl Acad Sci U S A 2003; 100: 1902-1907.

Raivich G, Gehrmann J, Kreutzberg GW: Increase of macrophage colony-stimulating factor and granulocyte-macrophage colony-stimulating factor receptors in the regenerating rat facial nucleus. J Neurosci Res 1991; 30: 682-686.

Rasband MN, Kagawa T, Park EW, Ikenaka K, Trimmer JS: Dysregulation of axonal sodium channel isoforms after adult-onset chronic demyelination. J Neurosci Res 2003; 73: 465-470.

Readhead C, Schneider A, Griffiths I, Nave KA: Premature arrest of myelin formation in transgenic mice with increased proteolipid protein gene dosage. Neuron 1994; 12: 583-595.

Seki T, Arai Y: Expression of highly polysialylated NCAM in the neocortex and piriform cortex of the developing and the adult rat. Anat Embryol (Berl) 1991; 184: 395-401.

Shibasaki K, Nakahira K, Trimmer JS, Shibata R, Akita M, Watanabe S, Ikenaka K: Mossy fiber contact triggers the targeting of Kv4.2 potassium channels to dendrites and synapses in developing cerebellar granule neurons. J Nuerochem; *in press*.

Simons M, Kramer EM, Macchi P, Rathke-Hartlieb S, Trotter J, Nave KA, Schulz JB: Overexpression of the myelin proteolipid protein leads to accumulation of cholesterol and proteolipid protein in endosomes/lysosomes: implications for Pelizaeus-Merzbacher disease. J Cell Biol 2002; 157: 327-336.

Sistermans EA, de Coo RF, De Wijs IJ, Van Oost BA: Duplication of the proteolipid protein gene is the major cause of Pelizaeus-Merzbacher disease. Neurology 1998; 50: 1749-1754.

Soares S, von Boxberg Y, Ravaille-Veron M, Vincent JD, Nothias F: Morphofunctional plasticity in the adult hypothalamus induces regulation of polysialic acid-neural cell adhesion molecule through changing activity and expression levels of polysialyltransferases. J Neurosci 2000; 20: 2551-2557.

Southwood C, Gow A: Molecular pathways of oligodendrocyte apoptosis revealed by mutations in the proteolipid protein gene. Microsc Res Tech 2001; 52: 700-708.

Steinhoff T, Moritz E, Wollmer MA, Mohajeri MH, Kins S, Nitsch RM: Increased cystatin C in astrocytes of transgenic mice expressing the K670N-M671L mutation of the amyloid precursor protein and deposition in brain amyloid plaques. Neurobiol Dis 2001; 8: 647-654.

Takebayashi H, Yoshida S, Sugimori M, Kosako H, Kominami R, Nakafuku M, Nabeshima Y: Dynamic expression of basic helix-loop-helix Olig family members: implication of Olig2 in neuron and oligodendrocyte differentiation and identification of a new member, Olig3. Mech Dev 2000; 99: 143-148.

Taupin P, Ray J, Fischer WH, Suhr ST, Hakansson K, Grubb A, Gage FH: FGF-2-responsive neural stem cell proliferation requires CCg, a novel autocrine/paracrine cofactor. Neuron 2000; 28: 385-397.

Van Der Voorn P, Tekstra J, Beelen RH, Tensen CP, Van Der Valk P, De Groot CJ: Expression of MCP-1 by reactive astrocytes in demyelinating multiple sclerosis lesions. Am J Pathol 1999; 154: 45-51.

Vitry S, Avellana-Adalid V, Lachapelle F, Evercooren AB: Migration and multipotentiality of PSA-NCAM+ neural precursors transplanted in the developing brain. Mol Cell Neurosci 2001; 17: 983-1000.

Wilkinson DG: Whole-mount In Situ Hybridization of Vertebrate Embryos. Oxford, IRL Press, 1992.

Woodward K, Kendall E, Vetrie D, Malcolm S: Pelizaeus-Merzbacher disease: identification of Xq22 proteolipid-protein duplications and characterization of breakpoints by interphase FISH. Am J Hum Genet 1998; 63: 207-217.

Zhou Q, Wang S, Anderson DJ: Identification of a novel family of oligodendrocyte lineage-specific basic helix-loop-helix transcription factors. Neuron 2000; 25: 331-343.

Figure legends

Fig. 1. Late-onset progressive demyelination in the optic nerve of *Plp/-* mice.

Semi-ultrathin sections were made from optic nerves at 1M (A,B), 6M (C), 7M (D), 8M (E, F) of wild (A, F) and heterozygous (B-E) mice.

Abbreviations: Wt, wild mice; He, heterozygous mice.

Scale bar, 10μm in (A-F).

Fig. 2. Late-onset progressive demyelination in the corpus callosum of *Plp/-* mice.

Coronal sections of adult mouse brain was stained by Kluver-Barrera's (KB) staining. Note that myelin, which is stained by luxol fast blue, is disrupted in the corpus callosum of heterozygous brain at 8 months (G) compared with wild brain (F). (B-G) shows the high-power view corresponding to the black boxed area in (A). White boxes in (B) indicate examples of fields for cell counting in Fig. 3.

Abbreviations: cc, corpus callosum; Cx, cortex.

Scale bars, 500μm in (A); 100μm in (B-G).

Fig. 3. Cell accumulation in the corpus callosum of *Plp/-* mouse at 8 months.

Comparison of the cell number in the corpus callosum of *Plp/-* and wild-type control mice at 2, 4, and 8 months. Each bar represents the number of cells per mm^2 with SD derived from ten fields. Examples of the fields were indicated in Fig. 2B as white boxed areas.

Fig. 4. Demyelination is also confirmed by MBP immunostaining.

(A-D) MBP immunostaining was performed in coronal sections of 8 months brain. (C, D) show higher magnification. Note that normal MBP positive myelin is not present in the corpus callosum at 8 months. (E, F) HE staining was performed on the coronal sections of 8 months brain. Abbreviations: Wt, wild mice; He, heterozygous mice.

Scale bars, 50μm in (A, B); 10μm in (C, D); 20μm in (E, F).

Fig. 5. *Olig1* positive oligodendrocyte progenitors accumulate in the demyelinated lesion of *Plp/-* mice.

In situ hybridization using *Olig1* riboprobe was performed on parasagittal cryosections of adult brains at 2M (A, B), 4M (C, D) and 8M (E, F). *Olig1* is expressed in the OLPs at an adult stage. Accumulating OLPs are observed in the demyelinating corpus callosum of

Plp/- brain at 8 months (F) compared with that of wild mice (E). Boxed areas in (E) indicate examples of fields for cell counting.

Scale bar, 500μm in (A-F).

Fig. 6. *Sox10* positive oligodendrocyte progenitors accumulate in the demyelinated lesion of *Plp/-* mice.

In situ hybridization using *Sox10* riboprobe was performed on parasagittal cryosections of adult brains at 2M (A, B), 4M (C, D) and 8M (E, F). *Sox10* is expressed in the OLPs at an adult stage. Accumulating OLPs are observed in the demyelinating corpus callosum of *Plp/-* brain at 8 months (F) compared with that of wild mice (E).

Scale bar, 500μm in (A-F).

Fig. 7. Oligodendrocytes are not effectively produced from transplanted neurosphere in the demyelinating corpus callosum of *Plp/-* mice.

Neurospheres were prepared from E14.5-ganglionic eminence of GFP expressing transgenic mice embryos. Secondary neurospheres were transplanted into demyelinated corpus callosum of the *Plp/-* mice at 8 months. Coronal (A, B) and parasagittal (C, D) cryosections were immunostained by anti-GFP (Green) and anti-MBP (Red) antibodies.

(B) and (D) indicate the higher magnifications of (A) and (C), respectively. Most of the transplanted cells locate at the site of transplantation and seemed to differentiate into astrocytes judged from their morphology (B, D).

Scale bars, 500μm in (A, C); 50μm in (B); 100μm in (D).

Fig. 8. PSA-NCAM is up-regulated in reactive astrocytes in the chronic demyelinating lesions.

(A, C, E, G, I) PSA-NCAM immunostaining was performed on coronal cryosections using 12E3 antibody. (B, D, F, H) MBP immunostaining was also performed on adjacent sections. Note that PSA-NCAM is up-regulated in the corpus callosum of heterozygous mice at 10 months (G). (I) shows the higher magnifications corresponding to the black boxed area in (G).

Scale bars, 100μm in (A-H); 20μm in (I).

Fig. 9. PSA-NCAM is up-regulated in the demyelinating axon.

(A, C) PSA-NCAM immunostaining was performed on coronal cryosections using 12E3 antibody. (B, D) MBP immunostaining was also performed on adjacent sections. Note that PSA-NCAM is up-regulated in the corpus callosum of heterozygous mice at 8 months

(C). (E) shows the high-power view corresponding to the black boxed area in (C). Note that axonal fibers at corpus callosum are positively stained by anti-PSA-NCAM antibody (arrowheads in E).

Scale bars, 100μm in (A-D); 20μm in (E).

Fig. 10. Up-regulation of *PST* mRNA in the retina of *Plp/-* mice.

(A) RT-PCR analyses of synthetic enzymes of PSA, *PST,* using retinal mRNA extracted from wild-type (lanes 1, 3, 5) and *Plp/-* (lanes 2, 4) mice at 6.5days(lane 1), 2 (lanes 2 and 3) and 5 months (lanes 4 and 5). (B) To normalize for sample variation, the expression of GAPDH was also measured as an internal control. *PST* mRNA is up-regulated at 2 and 5 months.

Fig. 11. *Cystatin C* positive cells are increased in the *Plp/-* mice brain.

In situ hybridization using *cystatin C* riboprobe was performed on parasagittal cryosections of adult brains at 2M (A, B), 4M (C, D) and 8M (E, F). (G) shows double staining between *cystatin C* ISH and GFAP immunohistochemistry. Many double positive cells are observed.

Scale bars, 200μm in (A-F); 50μm in (G).

Fig. 12. Astrocytes are activated much earlier stage than massive demyelinating stage.

(A, B) GFAP immunostaining was performed on coronal cryosections. Note that reactive astrocyte are observed in the cortex of *Plp/-* mice even at 2 months (B) compared with that of wild mice (A). (G) and (H) show higher magnification of boxed area in (A, B) and (E, F), respectively. The black circles in (A) indicate examples of fields for cell counting in Fig. 13.

Scale bars, 250μm in (A-F); 20μm in (G, H).

Fig. 13. Number of GFAP positive astrocytes in the cortex of *Plp/-* mouse increase before massive demyelination.

Comparison of the number of GFAP positive cells in the cortex of the *Plp/-* and wild-type control mice at 2, 4, 10 months. Each bar represents the number per mm^2 of the cells with SD derived from counting cells in eight fields. Examples of the fields are shown in Fig. 12A as black circles.

Fig. 14. Distribution of *c-fms* positive microglial cells in the hippocampus and corpus callosum.

In situ hybridization using *c-fms* riboprobe was performed on parasagittal cryosections of adult brains at 2M (A, B), 4M (C, D) and 8M (E, F). c-fms is a receptor for M-CSF and expressed in microglial cells/brain macrophages in the CNS.

Scale bar, 200μm in (A-F).

Fig. 15. Distribution of *c-fms* positive microglial cells in the cerebellum.

c-fms positive microglial cells accumulate in the white matter of cerebellum during demyelination (B, D, F).

Scale bar, 500μm in (A-F).

Fig. 16. Expression of *DAP12* mRNA in the corpus callosum and hippocampus.

In situ hybridization using *DAP12* riboprobe was performed on parasagittal cryosections of adult brains at 2M (A, B), 4M (C, D) and 8M (E, F). *DAP12* is expressed in the activated microglias. Its expression is observed in the corpus callosum of *Plp/-* brain as early as 2 months (B), while no expression is observed in the wild brain throughout the life (A, C, E).

Scale bar, 200μm in (A-F).

Fig. 17. Expression of *DAP12* mRNA in the cerebellum.

DAP12 riboprobe sensitively detects activated microglial cells during demyelination (B, D, F). On the other hand, no *DAP12* positive cells are observed in the cerebellum throughout the life (A, C, E).

Scale bar, 500μm in (A-F).

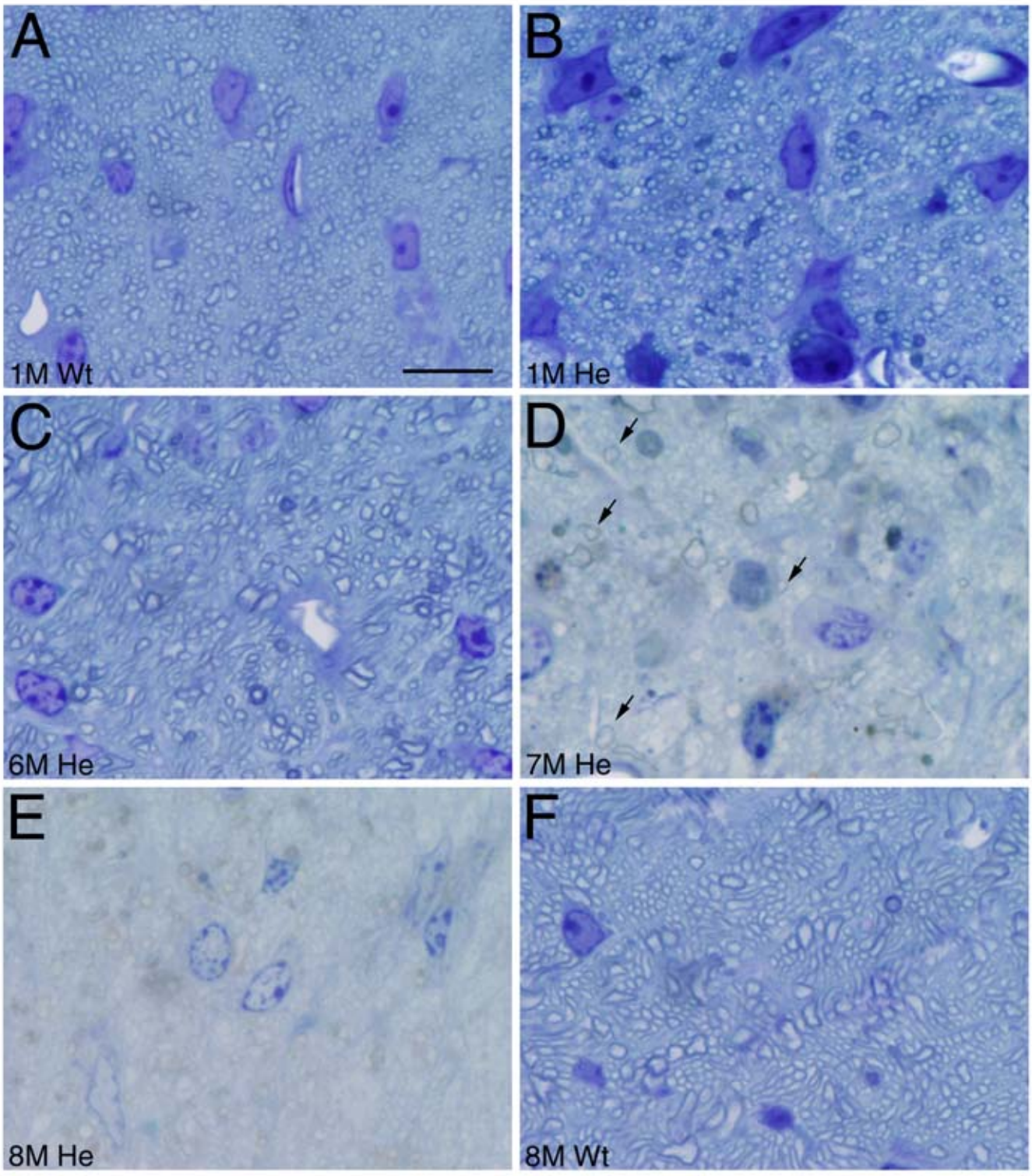

Fig. 1.

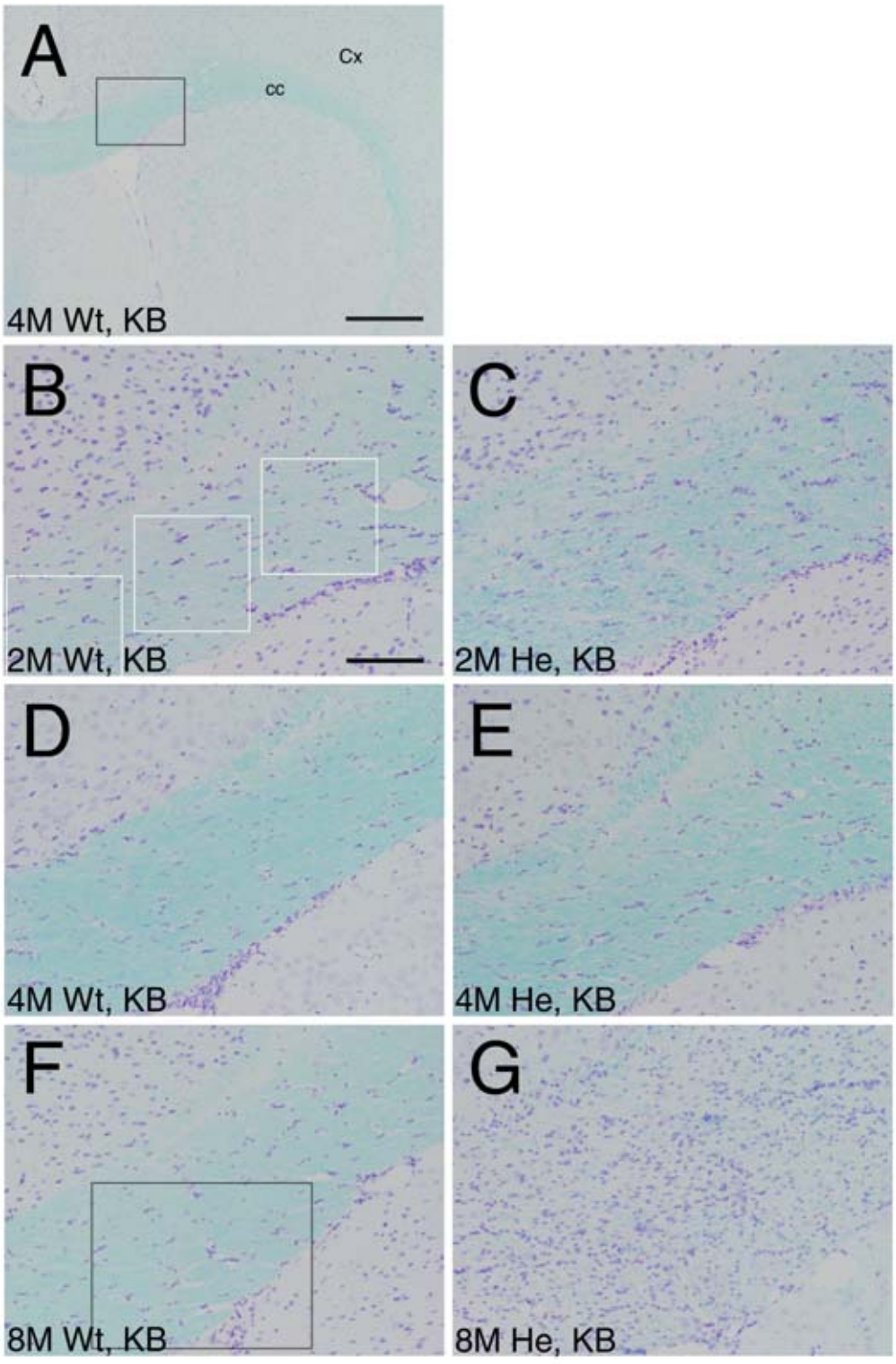
A
Cx
cc
4M Wt, KB
B
2M Wt, KB
C
2M He, KB
D
4M Wt, KB
E
4M He, KB
F
8M Wt, KB
G
8M He, KB

Fig. 2.

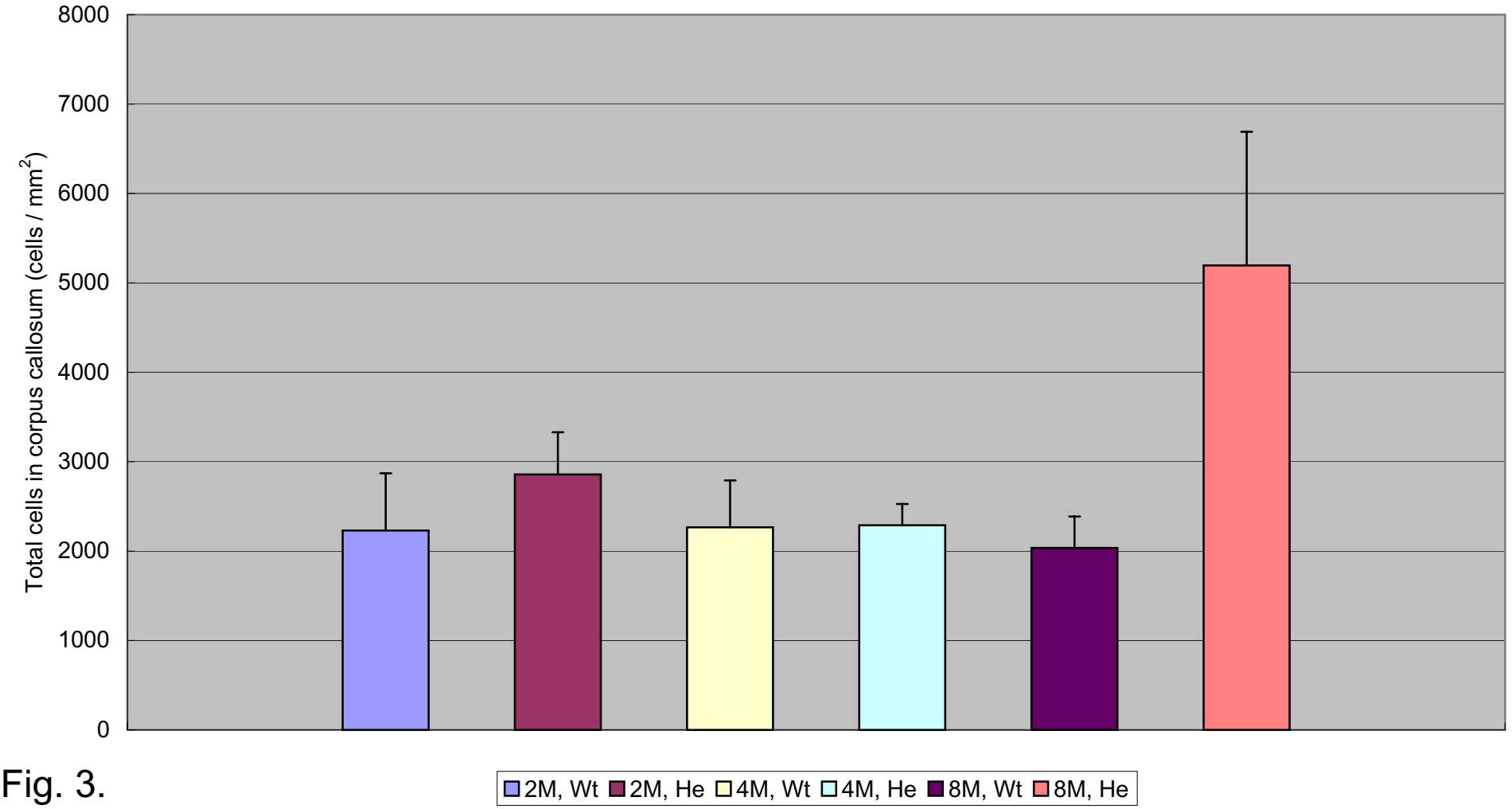
8000
7000
6000
5000
4000
3000
2000
1000
0
Total cells in corpus callosum (cells / mm2)
2M, Wt
2M, He
4M, Wt
4M, He
8M, Wt
8M, He

Fig. 3.

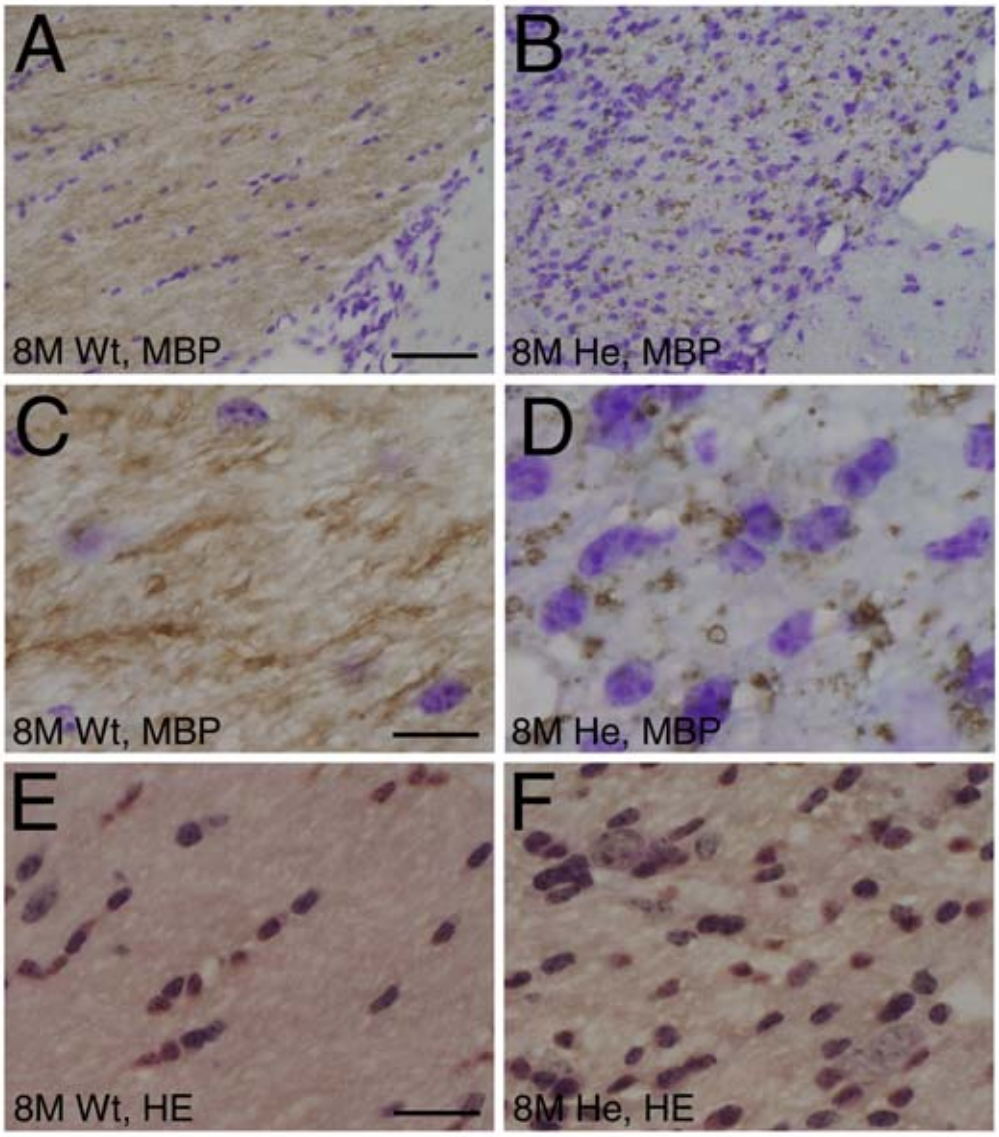

Fig. 4.

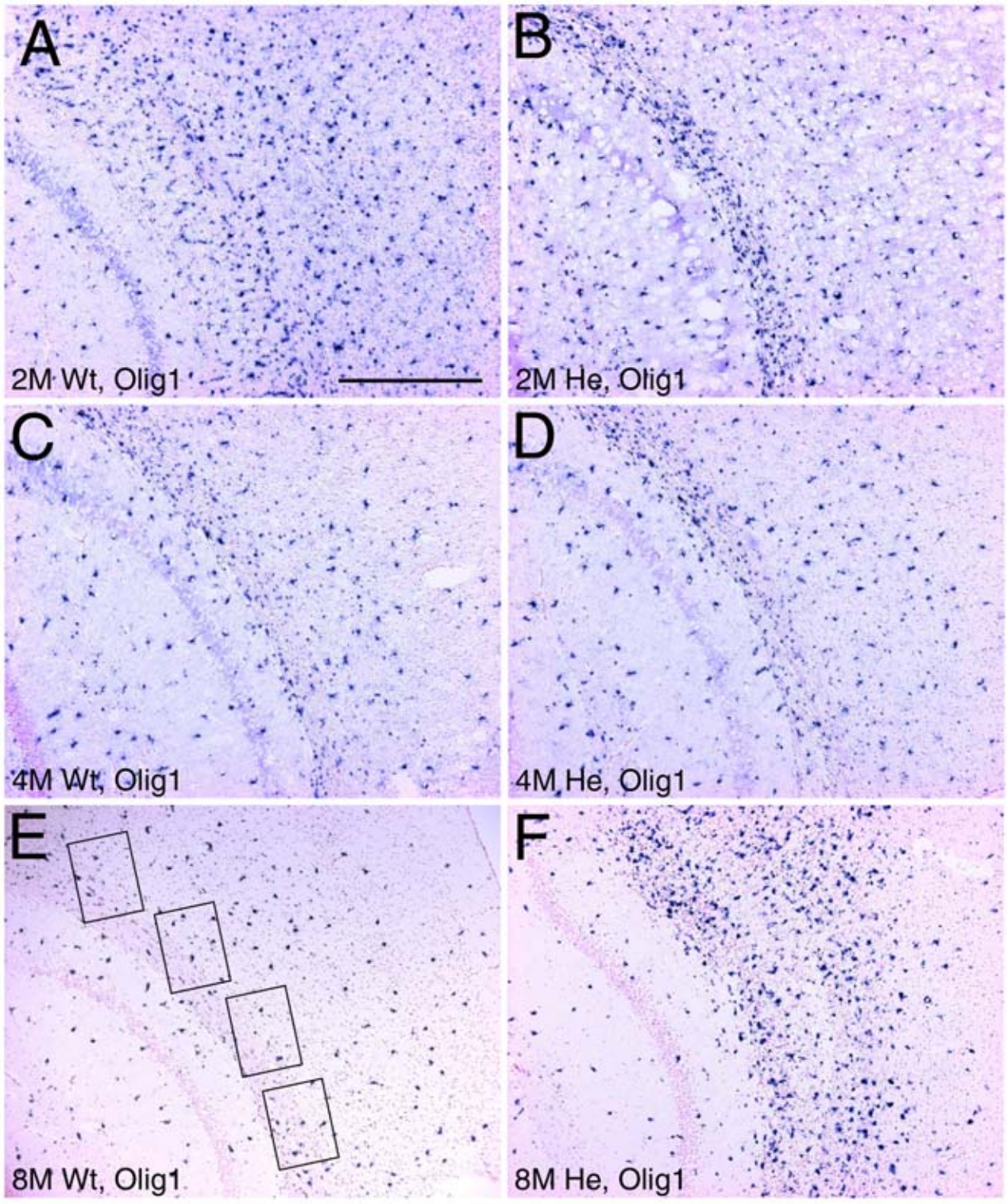
A
2M Wt, Olig1
B
2M He, Olig1
C
4M Wt, Olig1
D
4M He, Olig1
E
8M Wt, Olig1
F
8M He, Olig1

Fig. 5.

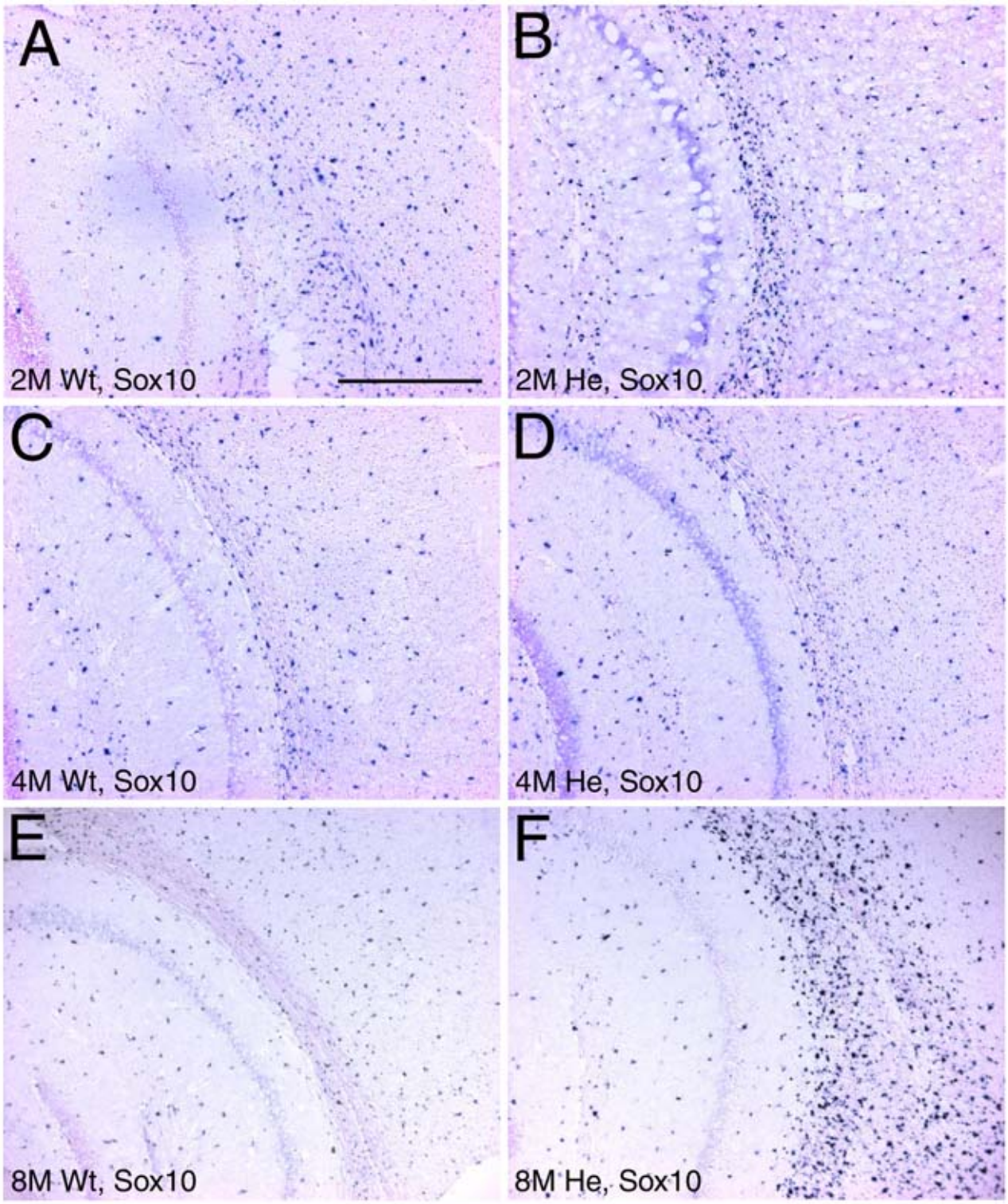
A
2M Wt, Sox10
B
2M He, Sox10
C
4M Wt, Sox10
D
4M He, Sox10
E
8M Wt, Sox10
F
8M He, Sox10

Fig. 6.

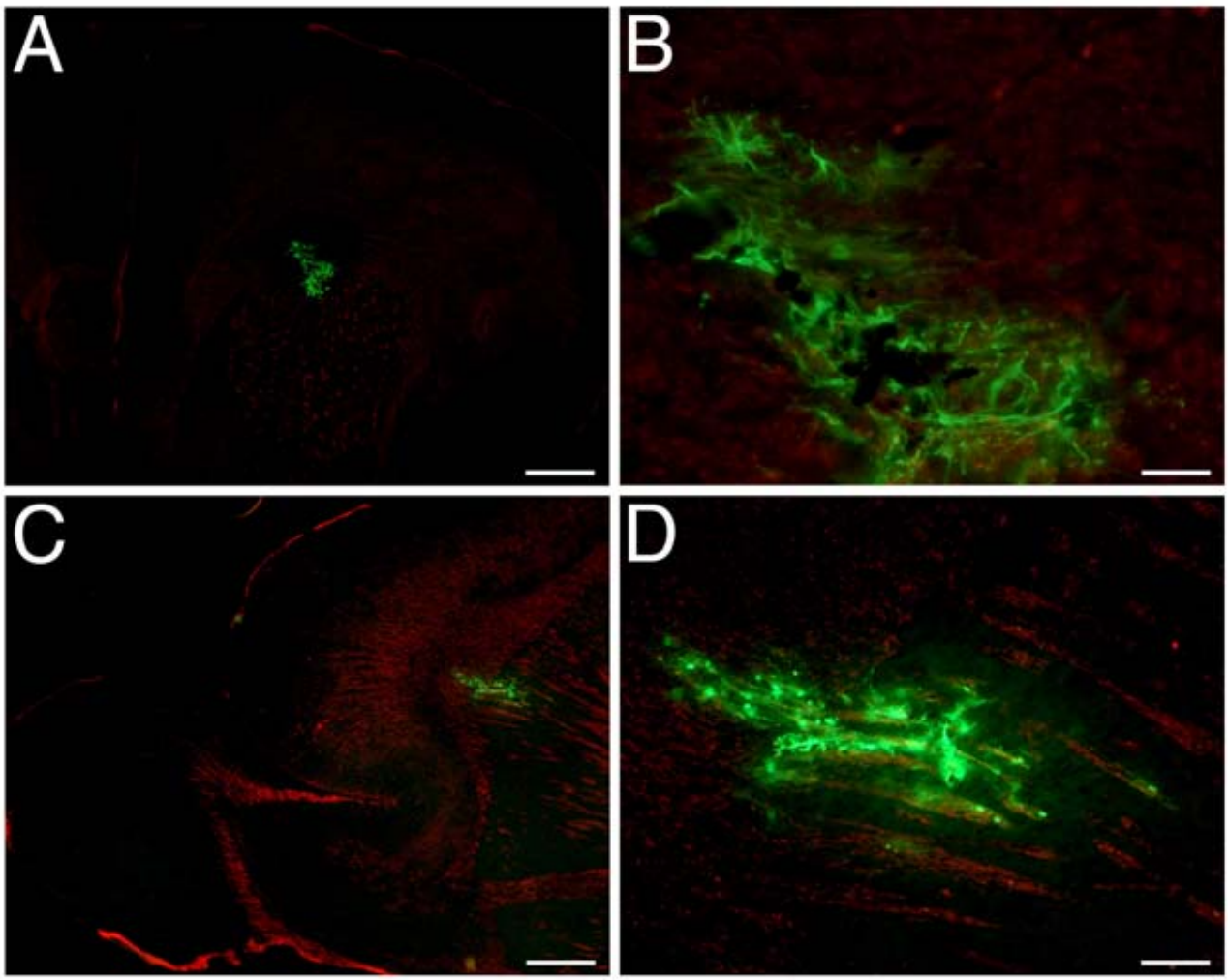

Fig. 7.

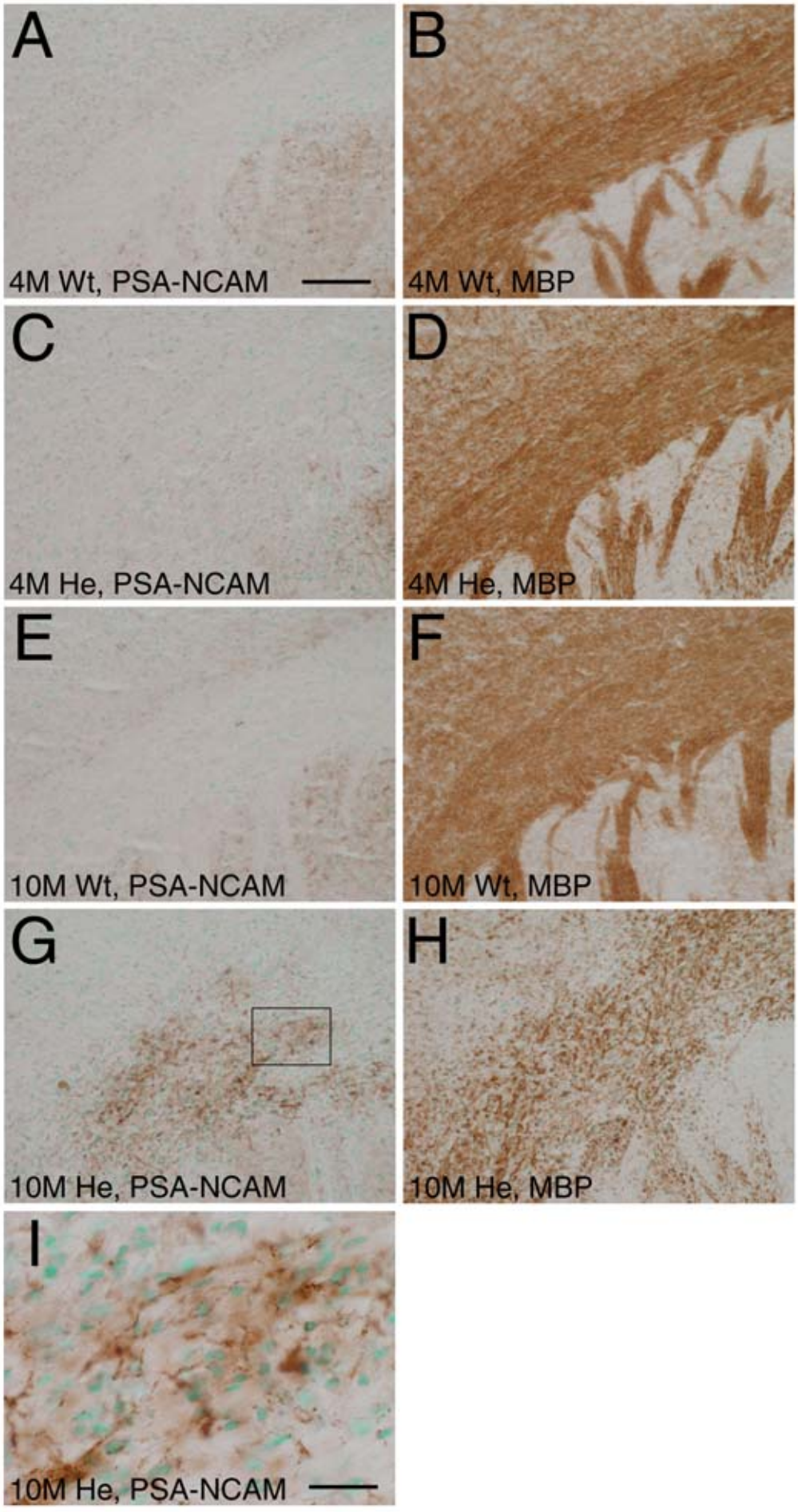
A
4M Wt, PSA-NCAM
B
4M Wt, MBP
C
4M He, PSA-NCAM
D
4M He, MBP
E
10M Wt, PSA-NCAM
F
10M Wt, MBP
G
10M He, PSA-NCAM
H
10M He, MBP
I
10M He, PSA-NCAM

Fig. 8.

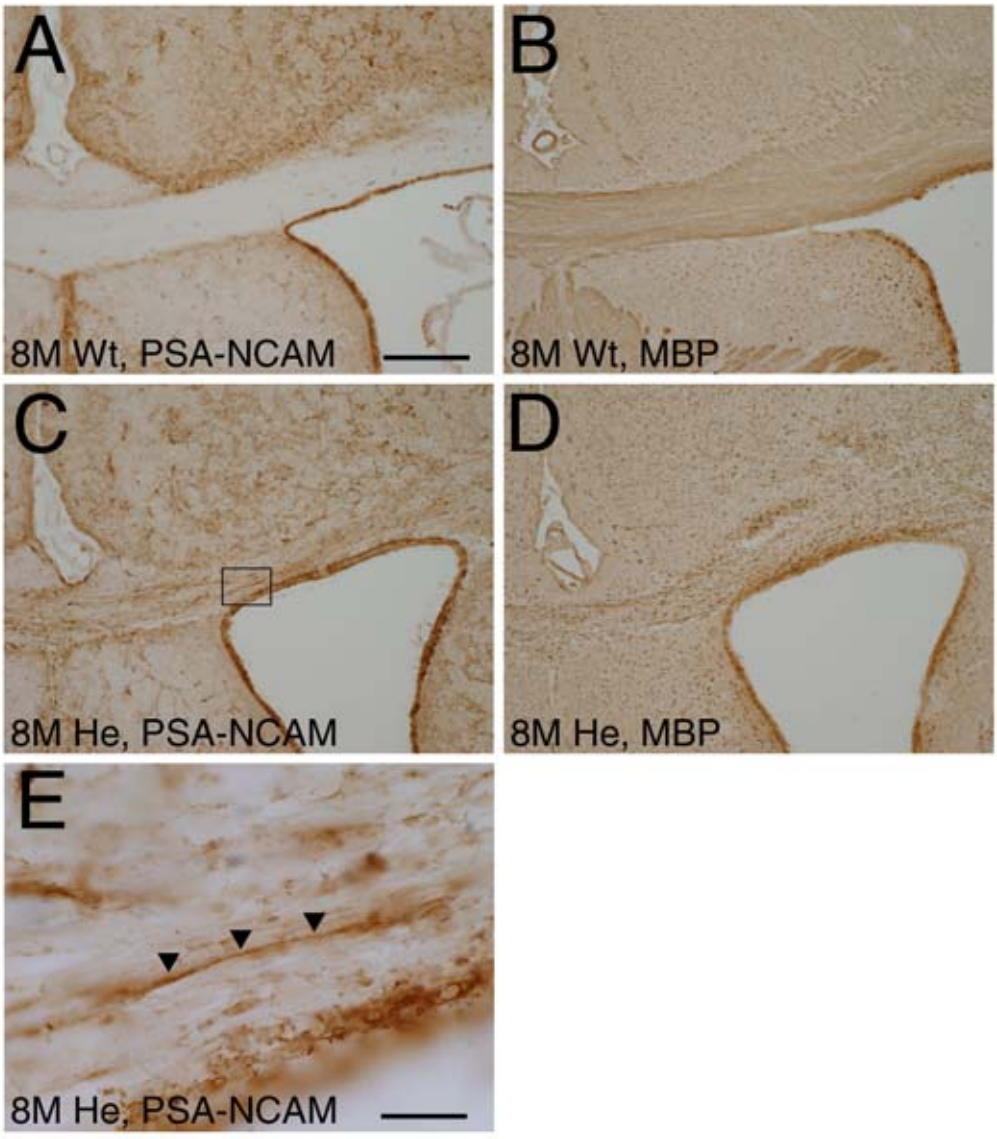
A
8M Wt, PSA-NCAM
B
8M Wt, MBP
C
8M He, PSA-NCAM
D
8M He, MBP
E
8M He, PSA-NCAM

Fig. 9.

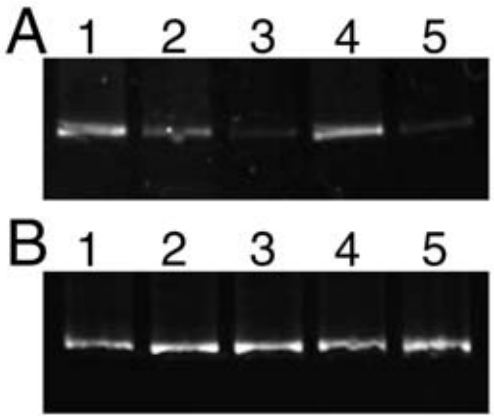

Fig. 10.

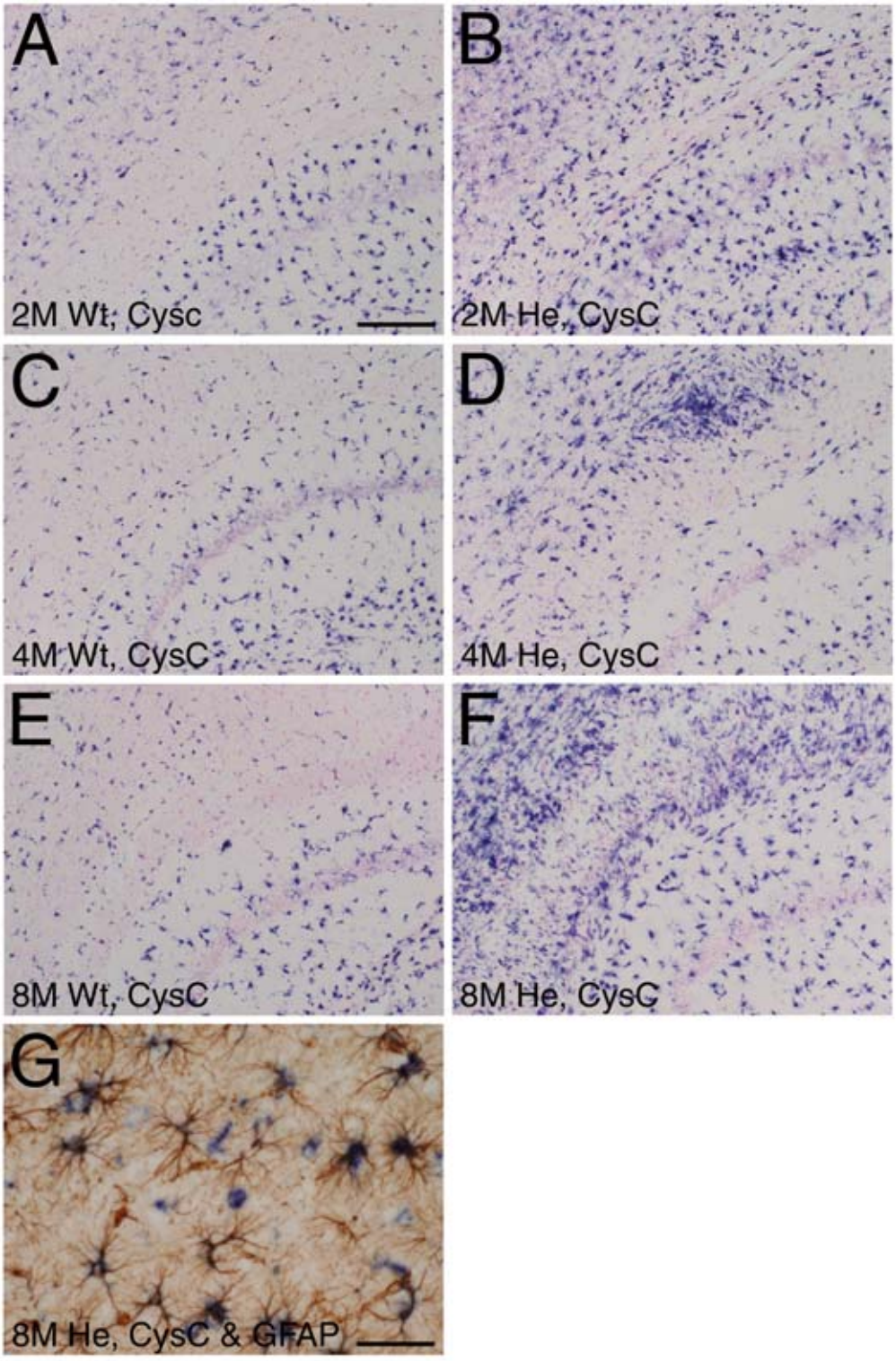
A
2M Wt, Cysc
B
2M He, CysC
C
4M Wt, CysC
D
4M He, CysC
E
8M Wt, CysC
F
8M He, CysC
G
8M He, CysC & GFAP

Fig. 11.

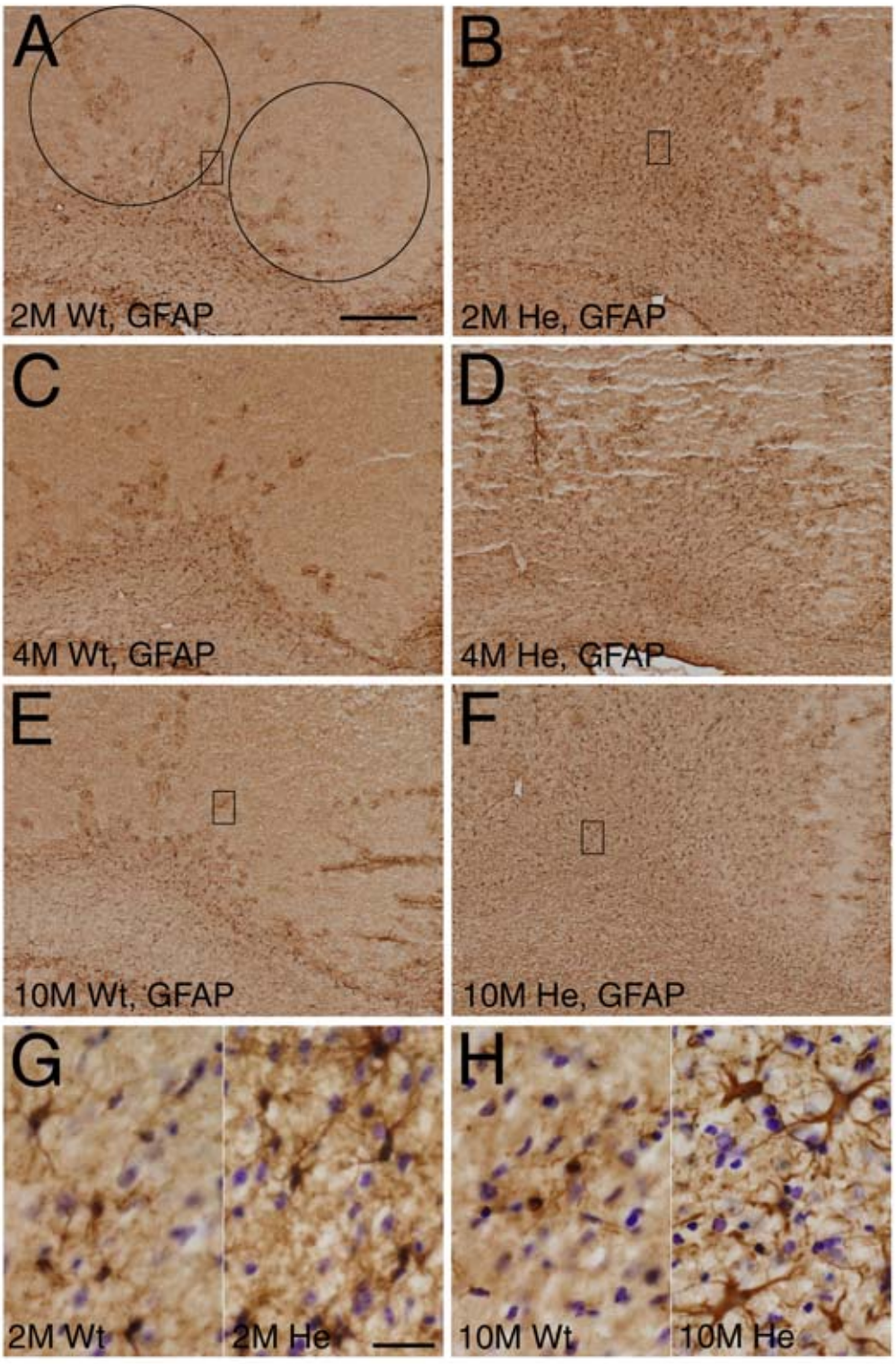
A
2M Wt, GFAP
B
2M He, GFAP
C
4M Wt, GFAP
D
4M He, GFAP
E
10M Wt, GFAP
F
10M He, GFAP
G
2M Wt
2M He
H
10M Wt
10M He

Fig. 12.

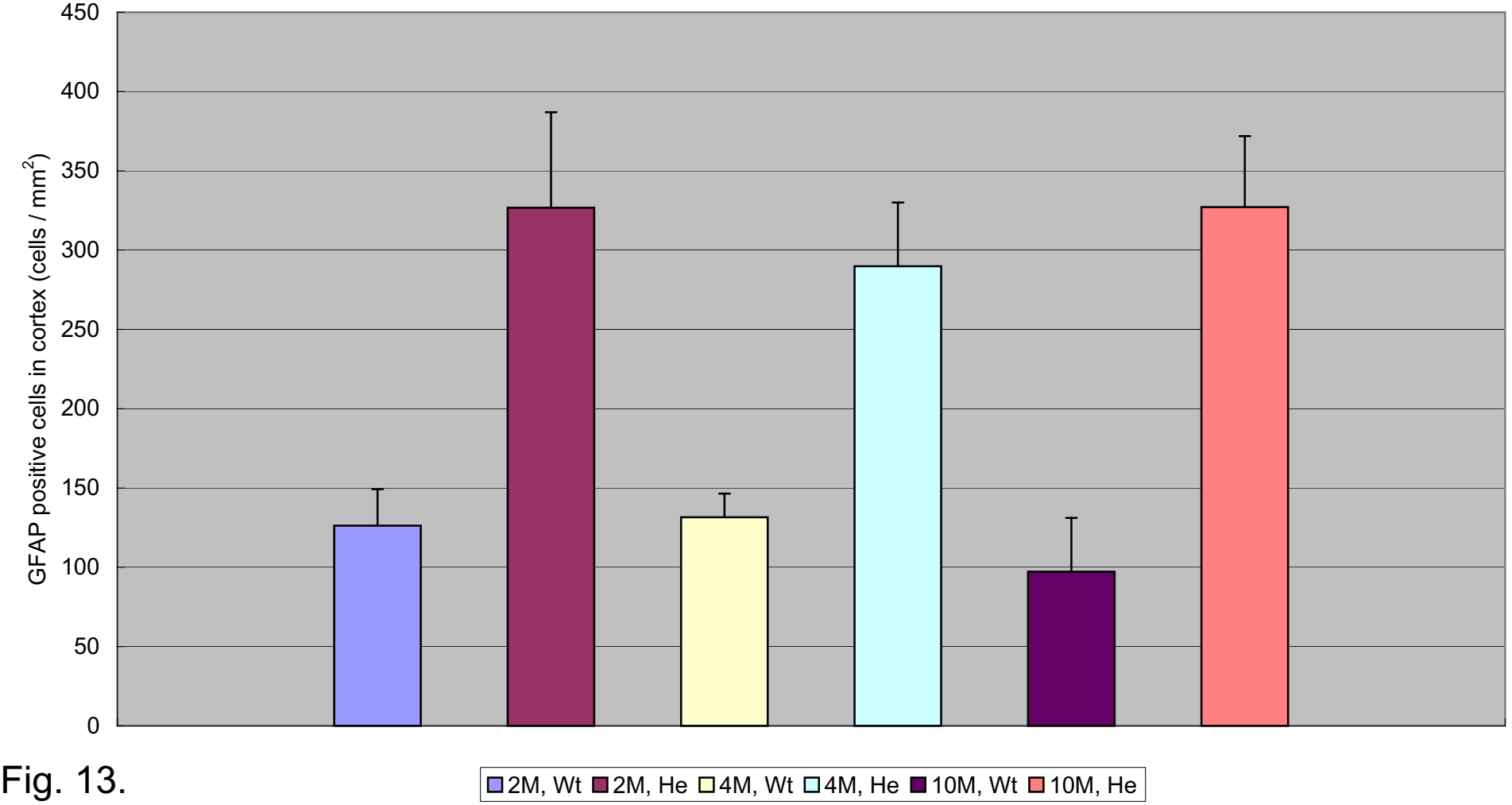
450
400
350
300
250
200
150
100
50
0
GFAP positive cells in cortex (cells / mm2)
2M, Wt
2M, He
4M, Wt
4M, He
10M, Wt
10M, He

Fig. 13.

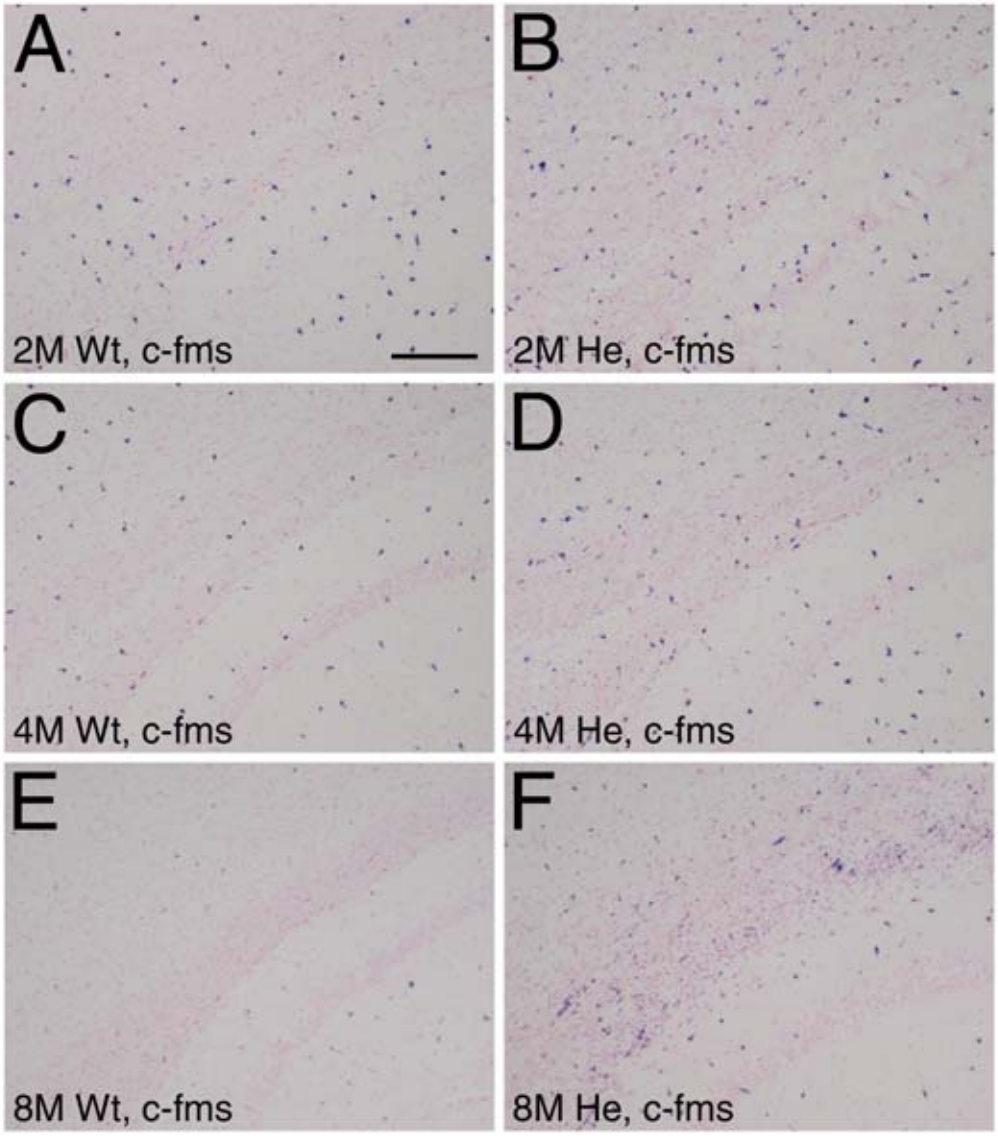
A
2M Wt, c-fms
B
2M He, c-fms
C
4M Wt, c-fms
D
4M He, c-fms
E
8M Wt, c-fms
F
8M He, c-fms

Fig. 14.

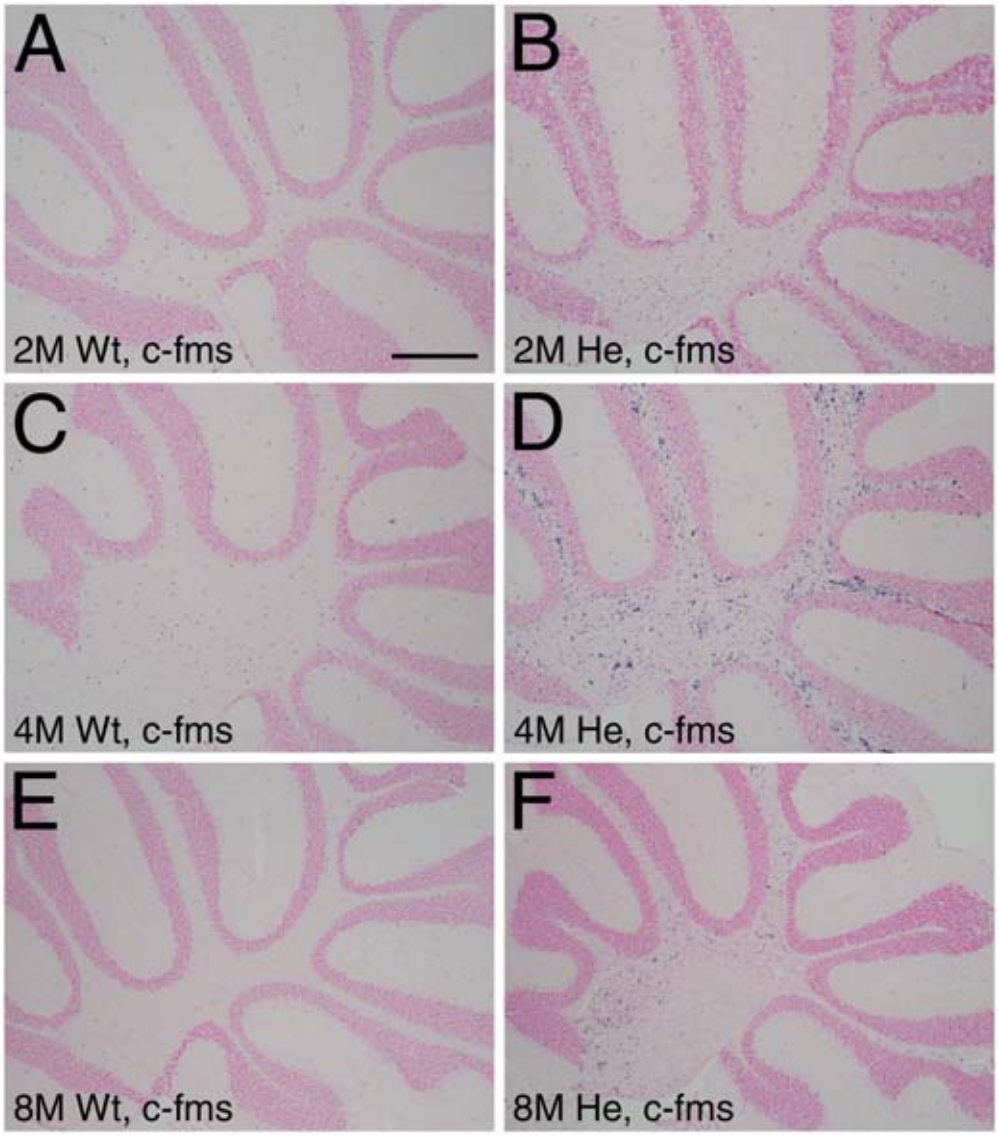
A
2M Wt, c-fms
B
2M He, c-fms
C
4M Wt, c-fms
D
4M He, c-fms
E
8M Wt, c-fms
F
8M He, c-fms

Fig. 15.

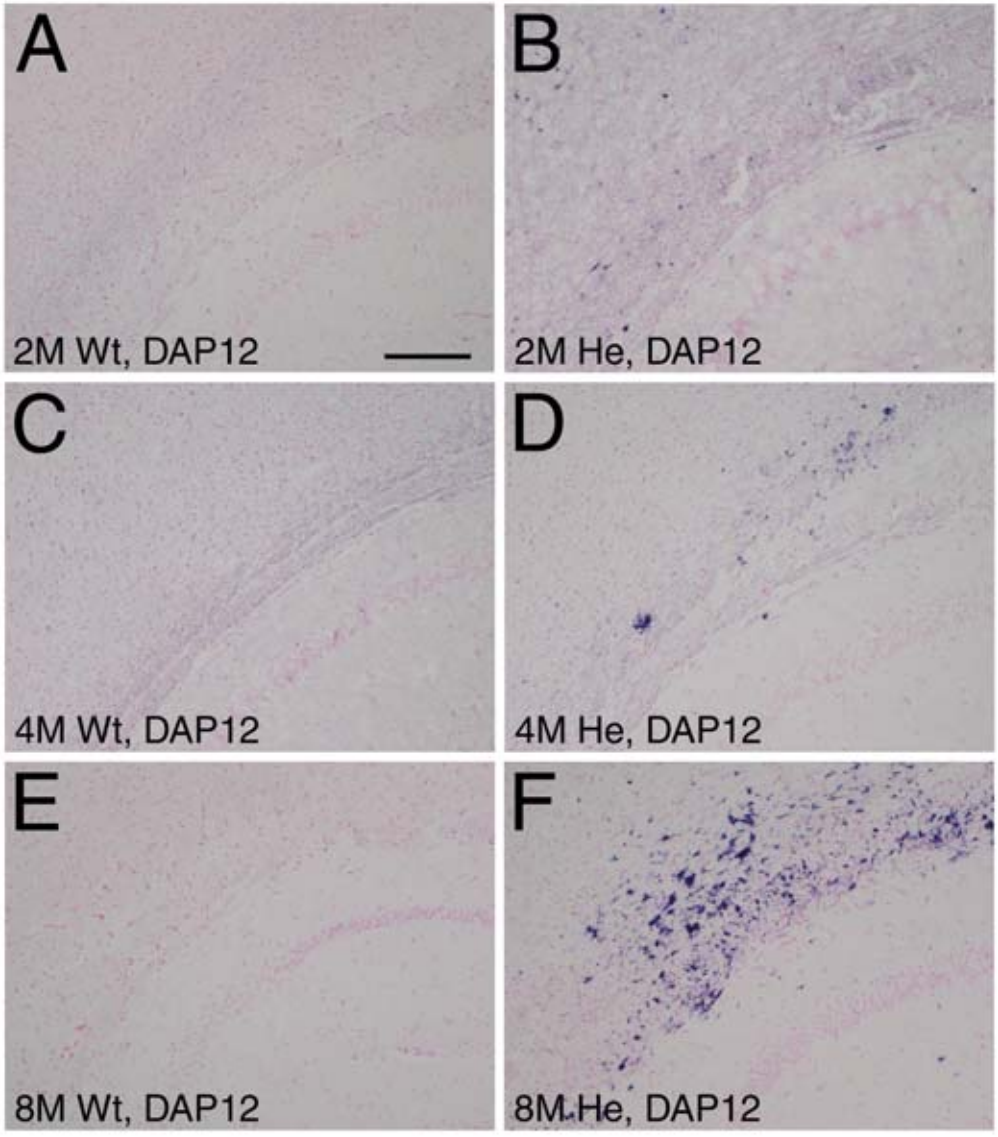
A
2M Wt, DAP12
B
2M He, DAP12
C
4M Wt, DAP12
D
4M He, DAP12
E
8M Wt, DAP12
F
8M He, DAP12

Fig. 16.

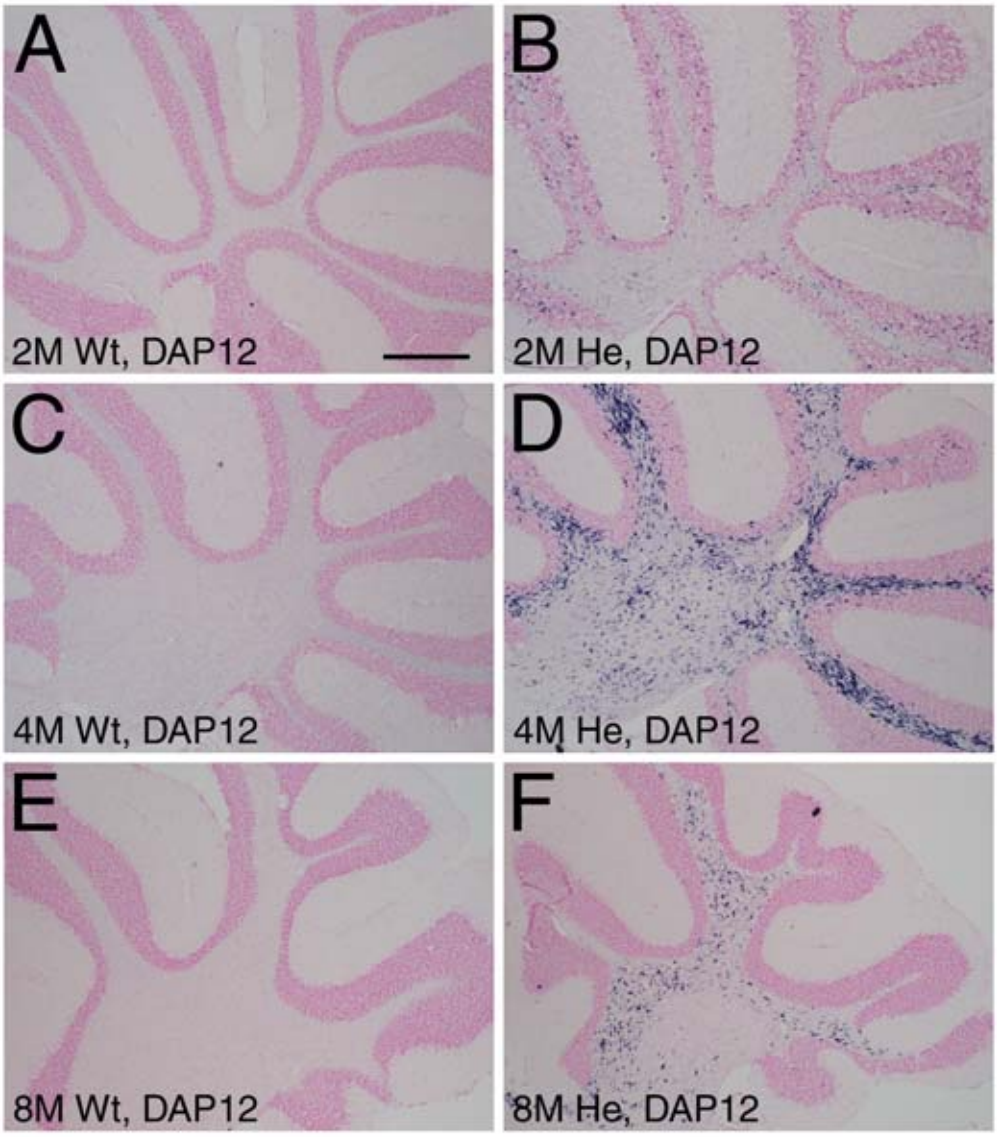
A
2M Wt, DAP12
B
2M He, DAP12
C
4M Wt, DAP12
D
4M He, DAP12
E
8M Wt, DAP12
F
8M He, DAP12

Fig. 17.